



UNIVERSITI PUTRA MALAYSIA

***STRUCTURAL, MAGNETIC AND MICROWAVE PROPERTIES OF
BISMUTH FERRITE CERAMIC WITH YTTRIUM SUBSTITUTION
PREPARED VIA MODIFIED THERMAL TREATMENT METHOD***

RAHIMAH BINTI MUSTAPA ZAHARI

FS 2022 26



**STRUCTURAL, MAGNETIC AND MICROWAVE PROPERTIES OF
BISMUTH FERRITE CERAMIC WITH YTTRIUM SUBSTITUTION
PREPARED VIA MODIFIED THERMAL TREATMENT METHOD**

RAHIMAH BINTI MUSTAPA ZAHARI

**Thesis Submitted to the School of Graduate Studies, Universiti Putra Malaysia, in
Fulfilment of the Requirements for the Degree of Doctor of Philosophy**

December 2021

All material contained within the thesis, including without limitation text, logos, icons, photographs and all other artwork, is copyright material of Universiti Putra Malaysia unless otherwise stated. Use may be made of any material contained within the thesis for non-commercial purposes from the copyright holder. Commercial use of material may only be made with the express, prior, written permission of Universiti Putra Malaysia.

Copyright © Universiti Putra Malaysia



DEDICATION

In appreciation of their love, doa', sacrifice, encouragement, advice, help, and support,
this thesis is dedicated to my beloved family. They are my parent, my husband, my
daughter, my son and my siblings.

*Maznah Binti Mohamed Noor
Mustapa Zahari Bin Mohamad Yusof*

*MD Farid Bin MD Asni
Nur Fatihah Binti MD Farid
Muhammad Al-Fatih Bin MD Farid*

*Muhammad Fauzi Bin Mustapa Zahari
Roslina Binti Mustapa Zahari
Muhammad Alif Bin Mustapa Zahari*

Abstract of thesis presented to the Senate of Universiti Putra Malaysia in fulfilment of
the requirement for the degree of Doctor of Philosophy

**STRUCTURAL, MAGNETIC AND MICROWAVE PROPERTIES OF
BISMUTH FERRITE CERAMIC WITH YTTRIUM SUBSTITUTION
PREPARED VIA MODIFIED THERMAL TREATMENT METHOD**

By

RAHIMAH BINTI MUSTAPA ZAHARI

December 2021

Chair : Professor Abdul Halim Bin Shaari, PhD
Faculty : Science

Bismuth ferrite (BiFeO_3 or BFO) with a perovskite structure is one of the multiferroic materials that shows simultaneous coexistence of antiferromagnetic and ferroelectric properties at room temperature, with antiferromagnetic Néel temperature, $T_N \sim 370$ °C and ferroelectric Curie temperature, $T_C \sim 820\text{--}850$ °C. Based on previous reports, bulk BFO suffers from high impurity phase due to the difficulty in synthesizing single-phase polycrystalline BFO because of the narrow range stability of temperature region, and weak magnetism. Although BFO materials have been extensively studied in the past few years, there are only few reports on Yttrium (Y) substitution at the Fe-site of BFO system. This thesis reports the effect of Y substitution on the structural, magnetic, and microwave properties of BFO. Also, the effect of different prepared temperatures was studied. Y-substituted bismuth ferrites ($\text{BiFe}_{1-x}\text{Y}_x\text{O}_3$ with $x = 0.0, 0.1, 0.2, 0.3, 0.4$ and 0.5) ceramics were synthesized via modified thermal treatment method. Three series of samples (or sample batches) were synthesized via modified thermal treatment method. The samples were calcined at 550 °C and sintered at three different temperatures. Batch-1 samples, Batch-2 samples and Batch-3 samples were sintered at 600 °C, 650 °C and 700 °C, respectively. The structural, magnetic and microwave properties of $\text{BiFe}_{1-x}\text{Y}_x\text{O}_3$ samples were characterized by X-ray diffraction (XRD), field emission scanning electron microscopy (FESEM), vibrating-sample magnetometer (VSM), and microwave network analyzer (MNA).

The XRD analysis showed that the BFO sample was matched to rhombohedral structure with R3c space group. A structural transition has been found to occur with increasing Y concentration. For Batch-1 samples, the structural transition has occurred from rhombohedral R3c ($x = 0.0$) to orthorhombic Pnma ($x = 0.1\text{--}0.5$). For Batch-2 and Batch-3 samples, the structural transition has occurred from rhombohedral R3c ($x = 0.0\text{--}0.1$) to orthorhombic Pnma ($x = 0.2\text{--}0.4$), and finally to cubic Fm-3m ($x = 0.5$), respectively.

FESEM analysis showed clear grain boundaries with well-defined grain structures of BFO. Also, FESEM analysis revealed that Y substitution has decreased the grain sizes of BFO sample. For Batch-1, Batch-2 and Batch-3 samples, the grain sizes decreased from 165 nm to 38 nm; 201 nm to 56 nm and 354 nm to 90 nm, respectively. The highest value of grain size of about 354 nm was observed in the pure BFO sample from Batch-3. In general, the grain sizes of all the samples were increased with increasing sintering temperatures.

The magnetic analysis showed that sample $x = 0.2$ in each sample batches indicated the enhancement of saturation magnetization, M_s . The M_s value at $x = 0.2$ from Batch-1 and also from Batch-2 was 0.17 emu/g, meanwhile the M_s value at $x = 0.2$ from Batch-3 was 3.95 emu/g. The highest remnant magnetization, M_r value of about 1.21 emu/g was observed for sample $x = 0.2$ from Batch-3. Pure BFO sample from Batch-1 had the highest coercive force, H_c value of 146.08 Oe. The magnetic behavior of BFO samples changed from weak-ferromagnetic to antiferromagnetic with the increase of sintering temperatures. Also, with the increase of sintering temperatures, the hysteresis loops for samples $x = 0.1, 0.2, 0.3, 0.4$, and 0.5 became larger and the saturation magnetization increased.

The microwave properties of all the samples were measured by the MNA at the frequency range between 8 and 12 GHz (X-band). For the one-port method, both the magnitude and phase of the reflection coefficient is good because of the metal-backed termination at end of the sample which will give stronger combined reflection at the front face of the sample. The minimum reflection loss, RL_{min} of -8.60 dB at 10.54 GHz was observed for sample $x = 0.1$ from Batch-2 and -5.25 dB at 9.90 GHz for sample $x = 0.0$ from Batch-3. The 3 mm thick sample of the pure BFO which was sintered at 600 °C indicated the lowest RL of -19 dB at 8 GHz which is much higher compared to the pure BFO sample measured at the thickness of 1 mm. The RL_{min} reflects the microwave absorption properties of the prepared samples. Therefore, the results suggest that the microwave absorption properties of all the samples can be manipulated by changing the amount of yttrium substitution into BFO compound and the thickness of the samples. Also, the results suggest that sample $x = 0.2$ as the potential ferromagnetic applications which possess a high value of M_s making it suitable for the fast processing and higher data storage magnetoelectric random-access memories (MERAM) devices.

Abstrak tesis yang dikemukakan kepada Senat Universiti Putra Malaysia sebagai memenuhi keperluan untuk ijazah Doktor Falsafah

**CIRI-CIRI STRUKTUR, MAGNET DAN MIKROGELOMBANG SERAMIK
BISMUT FERIT DENGAN PENGGANTIAN YTTRIUM DISINTESIS
MELALUI KAEDAH RAWATAN SUHU YANG DIUBAHSUAI**

Oleh

RAHIMAH BINTI MUSTAPA ZAHARI

Disember 2021

Pengerusi : Profesor Abdul Halim Bin Shaari, PhD
Fakulti : Sains

Bismut ferit (BiFeO_3 atau BFO) dengan struktur perovskit adalah salah satu bahan multiferoik yang menunjukkan kewujudan bersama serentak sifat-sifat antiferomagnet dan feroelektrik pada suhu bilik, dengan suhu Néel antiferomagnet, $T_N \sim 370$ °C dan suhu Curie feroelektrik, $T_C \sim 820\text{-}850$ °C. Berdasarkan kajian-kajian yang lalu, BFO pukal mengalami kerencatan oleh fasa bendasing yang tinggi menyebabkan kesukaran dalam sintesis fasa-tunggal BFO polihabur kerana kestabilan julat rantau suhu yang sempit, dan kemagnetan yang lemah. Walaupun bahan-bahan BFO telah dikaji dengan meluas dalam beberapa tahun kebelakangan ini, hanya terdapat sedikit laporan mengenai penggantian Yttrium (Y) di tapak-Fe sistem BFO. Tesis ini melaporkan kesan-kesan penggantian Y terhadap sifat-sifat struktur, magnet dan mikrogelombang BFO. Juga, kesan suhu penyediaan yang berbeza dikaji. Seramik Y-gantian bismut ferit ($\text{BiFe}_{1-x}\text{Y}_x\text{O}_3$ dengan $x = 0.0, 0.1, 0.2, 0.3, 0.4$ dan 0.5) disintesisikan melalui kaedah rawatan suhu yang diubahsuai. Tiga siri sampel (atau kelompok sampel) disintesisikan melalui kaedah rawatan suhu yang diubahsuai. Sampel-sampel itu dikalsinkan pada 550 °C dan disinterkan pada tiga suhu yang berbeza. Sampel kelompok-1, sampel kelompok-2 dan sampel kelompok-3 masing-masing disinterkan pada suhu 600 °C, 650 °C dan 700 °C. Sifat-sifat struktur, magnet dan mikrogelombang sampel $\text{BiFe}_{1-x}\text{Y}_x\text{O}_3$ dicirikan oleh pembelauan sinar-X (XRD), mikroskopi elektron pengimbasan pancairan medan (FESEM), magnetometer sampel-bergetar (VSM), dan penganalisis rangkaian mikrogelombang (MNA).

Analisis XRD menunjukkan bahawa sampel BFO dipadankan dengan struktur rombohedron dengan kumpulan ruang $R\bar{3}c$. Peralihan struktur didapati berlaku dengan peningkatan kepekatan Y. Untuk sampel kelompok-1, peralihan struktur telah berlaku dari rombohedron $R\bar{3}c$ ($x = 0.0$) ke ortorombik $Pnma$ ($x = 0.1\text{-}0.5$). Untuk sampel-sampel kelompok-2 dan kelompok-3, peralihan struktur telah berlaku masing-masing dari rombohedron $R\bar{3}c$ ($x = 0.0\text{-}0.1$) ke ortorombik $Pnma$ ($x = 0.2\text{-}0.4$), dan akhirnya ke kubik $Fm\text{-}3m$ ($x = 0.5$).

Analisis FESEM menunjukkan sempadan butiran yang jelas dengan struktur butiran BFO yang didefinisikan dengan baik. Juga, analisis FESEM mendedahkan bahawa penggantian Y telah mengecilkan saiz butiran sampel BFO. Untuk kelompok-1, kelompok-2 dan kelompok-3, saiz butiran masing-masing mengecil dari 165 nm ke 38 nm; 201 nm ke 90 nm; dan 354 nm ke 90 nm. Nilai tertinggi saiz butiran diperhatikan sekitar 354 nm dalam sampel BFO tulen daripada kelompok-3. Secara umumnya, saiz butiran untuk kesemua sampel meningkat dengan peningkatan suhu-suhu pensinteran.

Analisis magnet menunjukkan bahawa sampel $x = 0.2$ di dalam setiap kelompok sampel menandakan peningkatan pemagnetan tenu, M_s . Nilai M_s pada $x = 0.2$ daripada kelompok-1 dan juga daripada kelompok-2 adalah 0.17 emu/g, sementara nilai M_s pada $x = 0.2$ daripada kelompok-3 ialah 3.95 emu/g. Nilai tertinggi kemagnetan baki, M_r kira-kira 1.21 emu/g telah diperhatikan pada sampel $x = 0.2$ daripada kelompok-3. Sampel BFO tulen daripada kelompok-1 mempunyai nilai daya paksa, H_c yang tertinggi sebanyak 146.08 Oe. Perilaku magnet sampel-sampel BFO berubah daripada feromagnet lemah kepada antiferromagnet dengan peningkatan suhu-suhu pensinteran. Juga, dengan peningkatan suhu-suhu pensinteran, gelang histeresis untuk sampel-sampel $x = 0.1$ hingga 0.5 menjadi lebih besar dan pemagnetan tenu meningkat.

Sifat-sifat mikrogelombang kesemua sampel telah diukur oleh MNA pada julat frekuensi di antara 8 dan 12 GHz (jalur-X). Untuk kaedah satu-port, kedua-dua magnitud dan fasa pekali pantulan adalah bagus kerana penamatan berbelakang-logam dekat hujung sampel di mana ianya akan memberikan pantulan tergabung yang lebih kuat pada muka depan sampel tersebut. Kehilangan pantulan minimum, RL_{min} sebanyak -8.60 dB pada 10.54 GHz diperhatikan untuk sampel $x = 0.1$ daripada kelompok-2 dan -5.25 dB pada 9.90 GHz untuk sampel $x = 0.0$ daripada kelompok-3. Sampel BFO tulen berketingkat 3 mm yang telah disinter pada 600 °C telah menunjukkan RL terendah sebanyak -19 dB pada 8 GHz di mana ianya lebih tinggi dibandingkan dengan sampel BFO tulen yang diukur pada ketebalan 1 mm. RL_{min} tersebut mencerminkan sifat-sifat penyerapan mikrogelombang terhadap sampel-sampel yang disediakan. Lantaran itu, keputusan mencadangkan bahawa sifat-sifat penyerapan mikrogelombang untuk kesemua sampel boleh dimanipulasi dengan mengubah jumlah penggantian yttrium ke dalam sebatian BFO dan ketebalan sampel-sampel tersebut. Juga, keputusan mencadangkan bahawa sampel $x = 0.2$ sebagai aplikasi feromagnet berkeupayaan yang memiliki nilai M_s yang tinggi membuatkan ianya sesuai untuk pemprosesan pantas dan peranti ingatan capaian-rawak magnetoelektrik (MERAM) storan data yang lebih tinggi.

ACKNOWLEDGEMENTS

In the name of Allah, Alhamdulillah (all praises be to Allah Ta'ala). Thank you Allah because YOU give me the strength and opportunities to do the PhD and to finish the study. First and foremost, thank you very much to my husband for giving me the permission to do the PhD. Secondly, thank you to Universiti Putra Malaysia (UPM) for giving me chances to do the PhD here. I would like to acknowledge the financial support from UPM for the Putra grant (vote no. 9496800) and for all the facilities provided. I would also like to thank the Ministry of Higher Education, Malaysia (KPT) for the Fundamental Research Grant Scheme (FRGS 5524554) and the financial support through myBrain15-MyPhD programme.

Special thanks to my supervisor, Prof. Dr. Abdul Halim B. Shaari for accepting me as his PhD student. Thank you so much to Prof. for your consideration, encouragement, guidance, help, knowledge sharing, advice, and time. You are always so helpful. My sincere appreciation and thanks to my co-supervisors, Assoc. Prof. Dr. Zulkifly B. Abbas and Dr. Ismayadi B. Ismail, thank you for the guidance, knowledge sharing, and moral supports given by both of you. Thank you so much to Assoc. Prof. Dr. Hussein Baqiah for helping me in the submission of paper. I really appreciate the effort you have contributed to my research work.

It was challenging where I have to struggle to finish my study while raising two kids at the same time. Thank you to my husband for taking care of them. I would also like to express my gratitude to my parent and my parent-in-law for the advice, moral support, and taking care of my children while I was busy having classes and completing the research works. I have also been faced with many obstacles in completing the PhD but Alhamdulillah, finally I have successfully overcome the challenge.

I would also like to express my thanks to my colleagues and our staffs from Superconductors' laboratory for the help, advice, and knowledge sharing. Thank you to all the staffs in the Physics Department and Institute of Nanoscience and Nanotechnology (ION2) for the services provided. To my friends who had successfully completed their PhD studies especially Nor Azila, Nurzilla, Zamratul Maisarah and Siti Nor Ain, thank you for the friendship, good moment, advice, and knowledge sharing when we were studying here. Thank you to all those people who have helped me directly and indirectly in completing the research work. Jazakallahu-khairan (May Allah reward you with goodness).

I always have the inquisitiveness to know and explore new things in science which is related to physics. The PhD programme is so meaningful and taught me to be a good and liable person especially in handling and balancing the time to study, and the bonding time with family. The roots of education are bitter, but the fruit is sweet as quoted by Aristotle.

This thesis was submitted to the Senate of Universiti Putra Malaysia and has been accepted as fulfilment of the requirement for the degree of Doctor of Philosophy. The members of the Supervisory Committee were as follows:

Abdul Halim Bin Shaari, PhD

Professor

Faculty of Science

Universiti Putra Malaysia

(Chairman)

Zulkifly Bin Abbas, PhD

Associate Professor

Faculty of Science

Universiti Putra Malaysia

(Member)

Ismayadi Bin Ismail, PhD

Research Fellow

Institute of Nanoscience and Nanotechnology

Universiti Putra Malaysia

(Member)

ZALILAH MOHD SHARIFF, PhD

Professor and Dean

School of Graduate Studies

Universiti Putra Malaysia

Date: 9 March 2022

Declaration by graduate student

I hereby confirm that:

- this thesis is my original work;
- quotations, illustrations and citations have been duly referenced;
- this thesis has not been submitted previously or concurrently for any other degree at any other institutions;
- intellectual property from the thesis and copyright of thesis are fully-owned by Universiti Putra Malaysia, as according to the Universiti Putra Malaysia (Research) Rules 2012;
- written permission must be obtained from supervisor and the office of Deputy Vice-Chancellor (Research and Innovation) before the thesis is published (in the form of written, printed or in electronic form) including books, journals, modules, proceedings, popular writings, seminar papers, manuscripts, posters, reports, lecture notes, learning modules or any other materials as stated in the Universiti Putra Malaysia (Research) Rules 2012;
- there is no plagiarism or data falsification/fabrication in the thesis, and scholarly integrity is upheld as according to the Universiti Putra Malaysia (Graduate Studies) Rules 2003 (Revision 2012-2013) and the Universiti Putra Malaysia (Research) Rules 2012. The thesis has undergone plagiarism detection software.

Signature: _____

Date: _____

Name and Matric No.: _____ Rahimah Binti Mustapa Zahari _____

Declaration by Members of Supervisory Committee

This is to confirm that:

- the research conducted and the writing of this thesis was under our supervision;
- supervision responsibilities as stated in the Universiti Putra Malaysia (Graduate Studies) Rules 2003 (Revision 2012-2013) are adhered to.

Signature:

Name of Chairman of
Supervisory
Committee:

Prof. Dr. Abdul Halim Bin Shaari

Signature:

Name of Member of
Supervisory
Committee:

Prof. Madya Dr. Zulkifly Bin Abbas

Signature:

Name of Member of
Supervisory
Committee:

Dr. Ismayadi Bin Ismail

TABLE OF CONTENTS

	Page
ABSTRACT	i
ABSTRAK	iii
ACKNOWLEDGEMENTS	v
APPROVAL	vi
DECLARATION	viii
LIST OF TABLES	xiv
LIST OF FIGURES	xvii
LIST OF ABBREVIATIONS	xxviii
LIST OF SYMBOLS	xxx
 CHAPTER	
1 INTRODUCTION	
1.1 Multiferroics	1
1.2 Bismuth Ferrite	2
1.3 Microwave Absorption as Part of Microwave Studies in BFO	2
1.4 Problem Statement	2
1.5 Research Objectives	4
1.6 Limitations	4
1.7 Chapter Organization	4
2 LITERATURE REVIEW	
2.1 BFO Multiferroic Material	6
2.2 Perovskite BFO Structure	6
2.3 Electrical Properties of BFO	9
2.4 Magnetic Properties of BFO	9
2.5 Methods in Synthesizing BFO	10
2.5.1 Solid-State Method	10
2.5.2 Wet Chemical Method	13
2.6 Phase Diagrams	20
2.6.1 Phase Formation of BFO	20
2.6.2 Phase Formation of $\text{Bi}_{1-x}\text{La}_x\text{FeO}_3$ Solid Solution	21
2.7 General Problems Related to BFO	22
2.8 BFO Doping/Substitution	23
2.8.1 Doping/Substitution at Bi-sites of BFO system	23
2.8.2 Doping/Substitution at Fe-sites of BFO system	26
2.8.3 Co-doping/substitution at the Bi and Fe-sites of BFO system	27
2.9 Structural or Phase Analysis	29
2.10 Morphological Analysis	30
2.11 Magnetic Analysis	31

2.12	Microwave Techniques for Reflection/Transmission Measurement	32
2.12.1	Coaxial Line or Closed Waveguide Technique	33
2.12.2	Free Space Method	34
2.13	Transmission/Reflection Technique	36
2.14	Microwave Absorption Studies of BFO	36
3	THEORY	
3.1	Origin of Magnetism	39
3.2	Atoms as Magnets	39
3.3	Magnetic Properties of Matter	40
3.4	Magnetization in Materials	41
3.5	Classification of Magnetic Materials	42
3.5.1	Diamagnetism	43
3.5.2	Paramagnetism	44
3.5.3	Ferromagnetism	45
3.5.4	Antiferromagnetism	46
3.5.5	Ferrimagnetism	48
3.6	<i>M-H</i> Hysteresis Loop	48
3.6.1	Soft and Hard Magnetic Material	50
3.7	Polarization in Dielectrics	51
3.7.1	Dielectric Constant	51
3.7.2	Complex Permittivity and Permeability	52
3.7.3	Mechanism of Dielectric Polarization	53
3.8	Ferroelectricity	56
3.8.1	Ferroelectric Behavior	57
3.8.2	Ferroelectricity in BFO	57
3.9	Mechanism of Multiferroic	58
3.9.1	Lone-Pair Mechanism	60
3.9.2	Geometric Ferroelectricity	60
3.9.3	Charge Ordering	61
3.9.4	Spin-Driven Mechanism	61
3.10	Wave Equation	62
3.11	Calculation of the Reflection and Transmission Coefficient	63
3.12	Nicholson-Ross-Weir Method	66
3.13	Half-Wavelength Effect due to Sample Thickness Effect	67
3.14	Microwave Absorption	68
4	METHODOLOGY	
4.1	An Overview of Sample Preparation	70
4.1.1	Raw Materials	71
4.1.2	Mixing Process	72
4.1.3	Drying Process	72
4.1.4	Grinding Process	72
4.1.5	Calcination and Sintering Process	72
4.1.6	Pelletization Process	74
4.2	Characterization Process	74

4.2.1	Thermogravimetric Analysis	75
4.2.2	X-Ray Diffraction	76
4.2.3	Field Emission Scanning Electron Microscope	77
4.2.4	Energy-dispersive X-ray	78
4.2.5	Vibrating Sample Magnetometer	78
4.2.6	Microwave Network Analyzer	79
5	RESULTS AND DISCUSSIONS	
5.1	Formation of BFO Nanoparticles	82
5.2	TGA Analysis	83
5.3	XRD Analysis	85
5.3.1	Structural and phase analysis in each batch samples	85
5.3.2	Lattice parameters	94
5.3.3	Crystallite sizes	97
5.3.4	XRD patterns at different temperatures	98
5.4	FESEM and EDX Analysis	105
5.4.1	Effects of Y-substitution	105
5.4.2	Effects of sintering temperatures	111
5.5	Magnetic Studies	114
5.5.1	Effects of Y-substitution	114
5.5.2	Effects of sintering temperatures	122
5.5.3	Magnetization <i>vs.</i> Y-concentration at selected magnetic field	130
5.6	Microwave Properties	133
5.6.1	Complex relative permittivity measurement	133
5.6.2	Complex relative permeability measurement	137
5.6.3	Two-port Transmision and Reflection Method	142
5.6.4	Reflection measurement	148
5.6.5	Complex relative permittivity at different sintering temperatures	154
5.6.6	Complex relative permeability at different sintering temperatures	156
5.6.7	Magnitude and phase of the reflection and transmission coefficient at different sintering temperatures	159
5.6.8	Magnitude of the reflection coefficient (dB) at different sintering temperatures	163
5.6.9	One-port reflection method for sample $x = 0.0$ with the thickness of $d = 3$ mm	165
5.6.10	Comparison of the magnitude of the reflection coefficient or reflection loss (dB) using the one-port technique of BFO samples measured at different thicknesses of 1 mm and 3 mm	166
6	CONCLUSION AND RECOMMENDATIONS FOR FUTURE RESEARCH	
6.1	Conclusion	169
6.2	Suggestion	171

REFERENCES	174
APPENDICES	197
BIODATA OF STUDENT	209
LIST OF PUBLICATIONS	210



LIST OF TABLES

Table		Page
2.1	The advantages and disadvantages of the solid-state reaction method	13
2.2	The advantages and disadvantages of the wet chemical method	20
2.3	Summary on researchers and preparation methods based on doping/substitution at the A-site of BFO system	24
2.4	List of research works based on doping/substitution at the B-site of BFO system	27
2.5	Summary on researchers and preparation methods of co-doping/substitution at the A-site and B-site of BFO system	29
2.6	Research works related to microwave absorption studies	38
3.1	Magnetic susceptibilities	42
4.1	The descriptions of $\text{BiFe}_{1-x}\text{Y}_x\text{O}_3$ samples	70
4.2	List of chemicals and their specifications	71
5.1	Mechanism reaction process at three different stages	83
5.2	Structural properties of Batch-1 samples	87
5.3	Structural phase percentages of Batch-1 samples obtained from Rietveld refinement analysis	87
5.4	Structural properties of Batch-2 samples	90
5.5	Structural phase percentages of Batch-2 samples obtained from Rietveld refinement analysis	91
5.6	Structural properties of Batch-3 samples	93
5.7	Structural phase percentages of Batch-3 samples obtained from Rietveld refinement analysis	94
5.8	EDX results for Batch-1 ceramics	107
5.9	EDX results for Batch-2 ceramics	109

5.10	EDX results for Batch-3 ceramics	111
5.11	Magnetic properties of sample $x = 0.0$ at different sintering temperatures	123
5.12	Magnetic properties of sample $x = 0.1$ at different sintering temperatures	125
5.13	Magnetic properties of sample $x = 0.2$ at different sintering temperatures	126
5.14	Magnetic properties of sample $x = 0.3$ at different sintering temperatures	127
5.15	Magnetic properties of sample $x = 0.4$ at different sintering temperatures	128
5.16	Magnetic properties of sample $x = 0.5$ at different sintering temperatures	129
6.1	Molar mass in each material	198
6.2	Results for the calculation in step iv	199
6.3	Results for the calculation in step v	199
6.4	Structural phase percentages obtained from Rietveld refinement analysis of sample $x = 0.0$ sintered at different temperatures	201
6.5	Structural phase percentages obtained from Rietveld refinement analysis of sample $x = 0.1$ sintered at different temperatures	201
6.6	Structural phase percentages obtained from Rietveld refinement analysis of sample $x = 0.2$ sintered at different temperatures	201
6.7	Structural phase percentages obtained from Rietveld refinement analysis of sample $x = 0.3$ sintered at different temperatures	202
6.8	Structural phase percentages obtained from Rietveld refinement analysis of sample $x = 0.4$ sintered at different temperatures	202
6.9	Structural phase percentages obtained from Rietveld refinement analysis of sample $x = 0.5$ sintered at different temperatures	202
6.10	Comparison of the grain sizes, magnetic properties, and the minimum reflection loss values in sample $x = 0.0$ at different sintering temperatures	203

6.11	Comparison of the grain sizes, magnetic properties, and the minimum reflection loss values in sample $x = 0.1$ at different sintering temperatures	203
6.12	Comparison of the grain sizes, magnetic properties, and the minimum reflection loss values in sample $x = 0.2$ at different sintering temperatures	203
6.13	Comparison of the grain sizes, magnetic properties, and the minimum reflection loss values in sample $x = 0.3$ at different sintering temperatures	203
6.14	Comparison of the grain sizes, magnetic properties, and the minimum reflection loss values in sample $x = 0.4$ at different sintering temperatures	203
6.15	Comparison of the grain sizes, magnetic properties, and the minimum reflection loss values in sample $x = 0.5$ at different sintering temperatures	203
6.16	Grain sizes, magnetic properties, minimum reflection loss, and frequency of minimum reflection loss in Batch-1 samples at different Y-concentrations	204
6.17	Grain sizes, magnetic properties, minimum reflection loss, and frequency of minimum reflection loss in Batch-2 samples at different Y-concentrations	204
6.18	Grain sizes, magnetic properties, minimum reflection loss, and frequency of minimum reflection loss in Batch-3 samples at different Y-concentrations	204

LIST OF FIGURES

Figure		Page
1	Schematic diagram of multiferroic materials	1
2.1	Structure of (a) a perovskite with a chemical formula ABX_3 and (b) the calcium titanate oxide ($CaTiO_3$)	7
2.2	The structure of (a) a primitive unit cell of BFO and (b) rhombohedral distorted perovskite of BFO	7
2.3	BFO structure in the hexagonal unit cell along $[001]_h$ /pseudocubic unit cell along $[111]_c$	8
2.4	Portion of BFO lattice (the spiral period is reduced). The arrows indicate the Fe^{3+} moment direction of the proposed model by Sosnowska et al. (1982)	10
2.5	Schematic diagram of microwave sintering technique	12
2.6	Schematic diagram of the possible mechanism for the formation of BFO nanoparticles via a wet chemical route using (a) tartaric acid, and (b) citric acid as chelating agents. Colour: Purple for Bi-atoms, blue for Fe-atoms, red for O-atoms, and grey for C-atoms.	17
2.7	Formation of BFO nanoparticles using modified thermal treatment method	19
2.8	Bi_2O_3 - Fe_2O_3 phase diagram	21
2.9	Pseudo-binary $BiFeO_3$ - $LaFeO_3$ phase diagram	21
2.10	Slotted line technique to measure the complex permittivity of material	33
2.11	Measurement of sample X using an open-ended coaxial probe	34
2.12	Measurement of sample X using a free-space method	35
2.13	Dielectric waveguide technique	36
2.14	Transmission/reflection measurement using: (a) coaxial line, and (b) waveguide	36
2.15	Microwave absorption measurement using a metal-backed technique	37

3.1	Origin of magnetism; (a) orbital motion around the nucleus and (b) electron spinning	39
3.2	Circular current loop equivalents to the electronic motion of Figure 3.1(a)	40
3.3	Magnetic dipoles, (a) randomly oriented, and (b) magnetic dipoles oriented in the direction of the external field	40
3.4	Classification of magnetic materials	42
3.5	Properties of diamagnetic material; (a) no unpaired electrons, (b) very weakly repelled with a permanent magnet, (c) anti-parallel spin alignment with the magnetic field, and (d) external magnetic field bends slightly away from the material	43
3.6	The susceptibility of a diamagnetic material through (a) $M-H$ plot and (b) $\chi-T$ plot	44
3.7	Properties of paramagnetic material; (a) at least one unpaired electrons, (b) attracted with a permanent magnet, (c) parallel spin alignment with the magnetic field, and (d) external magnetic field bends toward the material	44
3.8	Paramagnetic material	45
3.9	Ferromagnetic material	45
3.10	Antiferromagnetic material	46
3.11	Types of antiferromagnetic spin structures	47
3.12	G-type antiferromagnetic spiral modulated spin structure	47
3.13	Ferrimagnetic material	48
3.14	The $M-H$ graph for diamagnetic, paramagnetic and antiferromagnetic materials	48
3.15	Hysteresis loop for a ferromagnetic material	49
3.16	Illustration of soft and hard magnetic materials	50
3.17	Mechanisms of electric polarization in dielectric materials	54
3.18	Variation in polarization with frequency	55
3.19	ABO_3 perovskite crystal structure	57

3.20	Crystal structure of bulk BFO with opposite rotation of successive oxygen octahedral around [111] polar axes. The red arrow indicates the orientation of Fe magnetic moments in the (111) plane	58
3.21	Types of multiferroics	59
3.22	Types of multiferroicity	59
3.23	Ferroelectricity due to lone-pair mechanism in BFO	60
3.24	Geometrically driven ferroelectricity in h-RMnO ₃	60
3.25	Ferroelectricity due to charge ordering in LuFeO ₃	61
3.26	Spin-driven mechanism by antisymmetric spin exchange interactions (inverse Dzyaloshinskii-Moriya interaction)	61
3.27	The reflection and transmission coefficients of a three-layered media	63
3.28	Variation in the magnitude of the (a) reflection coefficient, and (b) transmission coefficient of the three lossless samples ($\epsilon_r = 81, 9, \text{ and } 4$) with slab thickness at the frequency of 10 GHz	66
3.29	(a) Two-port measurement, (b) one-port measurement act as a short circuit	69
4.1	Flowchart of synthesizing and characterizing the BiFe _{1-x} Y _x O ₃ samples	71
4.2	Heating profile for calcination and sintering of BiFe _{1-x} Y _x O ₃ ($x = 0.0, 0.1, 0.2, 0.3, 0.4 \text{ and } 0.5$) samples	73
4.3	Schematic diagram of working principle of a thermogravimetric analyzer	75
4.4	Derivation of Bragg's law	76
4.5	Schematic diagram of a FESEM	77
4.6	Schematic diagram of the principle of the EDX	78
4.7	Schematic diagram of a VSM	79
4.8	Schematic diagrams of the (a) two-port and (b) one-port technique	79

4.9	Schematic diagrams of (a) measurement set-up of MNA and (b) dimension of a sample holder	80
5.1	Illustrations of mechanism interactions between the metallic ions and the amide groups using the thermal treatment method	82
5.2	(a) TGA and (b) DTG thermogram curves of BFO powder	84
5.3	XRD patterns of Batch-1 samples	85
5.4	XRD patterns of Batch-1 samples at $2\theta =$ (a) 21.75° to 23.50° , (b) 23.5° to 26.5° , (c) 27.25° to 28.75° , and (d) 31.0° to 34.5°	86
5.5	XRD patterns of Batch-2 samples	89
5.6	XRD patterns of Batch-2 samples at $2\theta =$ (a) 21.5° to 25.5° , (b) 27.0° to 29.0° , (c) 30.0° to 30.8° , and (d) 31.0° to 34.0°	90
5.7	XRD patterns of Batch-3 samples	92
5.8	XRD patterns of Batch-3 samples at $2\theta =$ (a) 22.0° to 23.5° , (b) 24.5° to 26.5° , (c) 27.0° to 29.5° , and (d) 31.5° to 33.5°	93
5.9	Lattice parameter of (a) a , (b) b , (c) c , and (d) volume of unit cell vs. Y concentration for Batch-1, Batch-2, and Batch-3 samples	95
5.10	Variation in tolerance factor with Y-concentrations for $\text{BiFe}_{1-x}\text{Y}_x\text{O}_3$ samples calculated using eq. (2.11)	96
5.11	Variation in the average crystallite sizes with Y-concentrations	97
5.12	XRD patterns of pure BFO sample sintered at different temperatures	99
5.13	XRD patterns of sample $x = 0.1$ at different sintering temperatures	100
5.14	XRD patterns of sample $x = 0.2$ at different sintering temperatures	101
5.15	XRD patterns of sample $x = 0.3$ at different sintering temperatures	102
5.16	XRD patterns of sample $x = 0.4$ at different sintering temperatures	103
5.17	XRD patterns of sample $x = 0.5$ at different sintering temperatures	104

5.18	FESEM images and EDX results of Batch-1 ceramics: (a) x = 0.0, (b) x = 0.1, (c) x = 0.2, (d) x = 0.3, (e) x = 0.4, and (f) x = 0.5	106
5.19	FESEM images and EDX results of Batch-2 ceramics: (a) x = 0.0, (b) x = 0.1, (c) x = 0.2, (d) x = 0.3, (e) x = 0.4, and (f) x = 0.5	108
5.20	FESEM images and EDX results of Batch-3 ceramics: (a) x = 0.0, (b) x = 0.1, (c) x = 0.2, (d) x = 0.3, (e) x = 0.4, and (f) x = 0.5	110
5.21	Variation in average grain sizes of $\text{BiFe}_{1-x}\text{Y}_x\text{O}_3$ ($x = 0.0, 0.1, 0.2, 0.3, 0.4$, and 0.5) ceramics with Y-concentrations	111
5.22	Comparison of micrograph images of pure BFO ceramics sintered at different temperatures	112
5.23	Comparison of micrograph images of sample $x = 0.1$ sintered at different temperatures	112
5.24	Comparison of micrograph images of sample $x = 0.2$ sintered at different temperatures	113
5.25	Comparison of micrograph images of sample $x = 0.3$ sintered at different temperatures	113
5.26	Comparison of micrograph images of sample $x = 0.4$ sintered at different temperatures	113
5.27	Comparison of micrograph images of sample $x = 0.5$ sintered at different temperatures	114
5.28	Room temperature M - H hysteresis loops of Batch-1 samples at (a) $x = 0.0$, (b) $x = 0.1$, (c) $x = 0.2$, (d) $x = 0.3$, (e) $x = 0.4$, (f) $x = 0.5$, (g) combined all samples, and (h) magnified M - H hysteresis loops of Batch-1 samples between -2 and 2 kOe	115
5.29	Coercivity (H_c), saturation magnetization (M_s), and remnant magnetization (M_r) of Batch-1 samples with Y-concentrations	116
5.30	Room temperature M - H hysteresis loops of Batch-2 samples at (a) $x = 0.0$, (b) $x = 0.1$, (c) $x = 0.2$, (d) $x = 0.3$, (e) $x = 0.4$, (f) $x = 0.5$, (g) combined all samples, and (h) magnified M - H hysteresis loops of Batch-2 samples between -1 and 1 kOe	117
5.31	Coercivity (H_c), saturation magnetization (M_s), and remnant magnetization (M_r) of Batch-2 samples with Y-concentrations	118

5.32	Room temperature M - H hysteresis loops of Batch-3 samples at (a) $x = 0.0$, (b) $x = 0.1$, (c) $x = 0.2$, (d) $x = 0.3$, (e) $x = 0.4$, (f) $x = 0.5$, (g) combined all samples, and (h) magnified M - H hysteresis loops of Batch-3 samples between -0.6 and 0.6 kOe	119
5.33	Coercivity (H_c), saturation magnetization (M_s), and remnant magnetization (M_r) of Batch-3 samples with Y-concentrations	120
5.34	Room temperature M - H hysteresis loops of pure BFO sample at different sintering temperatures	123
5.35	Room temperature M - H hysteresis loops of sample $x = 0.1$ at different sintering temperatures	124
5.36	Room temperature M - H hysteresis loops of sample $x = 0.2$ at different sintering temperatures	125
5.37	Room temperature M - H hysteresis loops of sample $x = 0.3$ at different sintering temperatures	127
5.38	Room temperature M - H hysteresis loops of sample $x = 0.4$ at different sintering temperatures	128
5.39	Room temperature M - H hysteresis loops of sample $x = 0.5$ at different sintering temperatures	129
5.40	Illustration of M - H curve at: (a) saturation point, (b) when the magnetic field is dropped to zero and (c) when the magnetic field is reversed and increased to drive the magnetization to zero	130
5.41	Variation in magnetization with Y-concentrations of Batch-1 samples at certain field	131
5.42	Variation in magnetization with Y-concentrations of Batch-2 samples at certain field	131
5.43	Variation in magnetization with Y-concentrations of Batch-3 samples at certain field	132
5.44	Variation in (a) dielectric constant, (b) dielectric loss factor, (c) and dielectric loss tangent with frequency of Batch-1 samples measured at thickness of $d = 1$ mm using the two-port technique	134
5.45	Variation in (a) dielectric constant, (b) dielectric loss factor, (c) and dielectric loss tangent with frequency of Batch-2 samples measured at thickness of $d = 1$ mm using the two-port	135

	technique	
5.46	Variation in (a) dielectric constant, (b) dielectric loss factor, (c) and dielectric loss tangent with frequency of Batch-3 samples measured at thickness of $d = 1$ mm using the two-port technique	135
5.47	Variation in (a) real part of permeability, (b) imaginary part of permeability, (c) and magnetic loss tangent with frequency of Batch-1 samples measured at thickness of $d = 1$ mm using the two-port technique	138
5.48	Variation in (a) real part of permeability, (b) imaginary part of permeability, (c) and magnetic loss tangent with frequency of Batch-2 samples measured at thickness of $d = 1$ mm using the two-port technique	138
5.49	Variation in (a) real part of permeability, (b) imaginary part of permeability, (c) and magnetic loss tangent with frequency of Batch-3 samples measured at thickness of $d = 1$ mm using the two-port technique	139
5.50	The eddy current loss vs. frequency plot for (a) Batch-1, (b) Batch-2 and (c) Batch-3 samples	141
5.51	(a) Magnitude of the reflection coefficient, $ \Gamma $ and transmission coefficient $ S_{21} $, and (b) phase of the reflection coefficient, ϕS_{11} and transmission coefficient, ϕS_{21} of the air	142
5.52	Variation in (a) magnitude, (b) normalized magnitude, (c) phase and (d) phase shift of reflection coefficient of Batch-1 samples with frequency measured at thickness of $d = 1$ mm using the two-port technique	143
5.53	Variation in (a) magnitude, (b) normalized magnitude, (c) phase, and (d) phase shift of transmission coefficient of Batch-1 samples with frequency measured at thickness of $d = 1$ mm using the two-port technique	144
5.54	Variation in (a) magnitude, (b) normalized magnitude, (c) phase, and (d) phase shift of reflection coefficient of Batch-2 samples with frequency measured at thickness of $d = 1$ mm using the two-port technique	145
5.55	Variation in (a) magnitude, (b) normalized magnitude, (c) phase, and (d) phase shift of transmission coefficient of Batch-2 samples with frequency measured at thickness of $d = 1$ mm using the two-port technique	146
5.56	Variation in (a) magnitude, (b) normalized magnitude, (c) phase	147

	and (d) phase shift of reflection coefficient of Batch-3 samples with frequency measured at thickness of $d = 1$ mm using the two-port technique	
5.57	Variation in (a) magnitude, (b) normalized magnitude, (c) phase and (d) phase shift of transmission coefficient of Batch-3 samples with frequency measured at thickness of $d = 1$ mm using the two-port technique	148
5.58	Illustration of the mechanism of microwaves interaction in the BFO samples using the one-port technique. (a) Part of the energy is reflected in the air and sample interface, (b) part of the energy is absorbed, and (c) part of the energy is reflected in the sample and metal interface	148
5.59	Variation in (a) magnitude, (b) normalized magnitude, (c) phase and (d) phase shift of reflection coefficient of Batch-1 samples with frequency measured at thickness of $d = 1$ mm using the one-port technique	150
5.60	Variation in (a) magnitude, and (b) normalized magnitude, (c) phase and (d) phase shift of reflection coefficient of Batch-2 samples with frequency measured at thickness of $d = 1$ mm using the one-port technique	151
5.61	Variation in (a) magnitude, and (b) normalized magnitude, (c) phase and (d) phase shift of reflection coefficient of Batch-3 samples with frequency measured at thickness of $d = 1$ mm using the one-port technique	152
5.62	A good illustration of the reflection phenomena of a metal-backed sample	154
5.63	Comparison of (a) dielectric constant, (b) dielectric loss, and (c) dielectric loss tangent with frequency of pure BFO sample at different sintering temperature	154
5.64	Comparison of (a) dielectric constant, (b) dielectric loss, and (c) dielectric loss tangent with frequency of sample $x = 0.1$ at different sintering temperature	155
5.65	Comparison of (a) dielectric constant, (b) dielectric loss, and (c) dielectric loss tangent with frequency of sample $x = 0.2$ at different sintering temperature	155
5.66	Comparison of (a) dielectric constant, (b) dielectric loss, and (c) dielectric loss tangent with frequency of sample $x = 0.3$ at different sintering temperature	155
5.67	Comparison of (a) dielectric constant, (b) dielectric loss, and (c)	155

	dielectric loss tangent with frequency of sample $x = 0.4$ at different sintering temperature	
5.68	Comparison of (a) dielectric constant, (b) dielectric loss, and (c) dielectric loss tangent with a frequency of sample $x = 0.5$ at different sintering temperature	156
5.69	Comparison of (a) real part of permeability, (b) imaginary part of permeability, and (c) magnetic loss tangent with frequency of the pure BFO sample at different sintering temperature	156
5.70	Comparison of (a) real part of permeability, (b) imaginary part of permeability, and (c) magnetic loss tangent with frequency of sample $x = 0.1$ at different sintering temperature	157
5.71	Comparison of (a) real part of permeability, (b) imaginary part of permeability, and (c) magnetic loss tangent with a frequency of sample $x = 0.2$ at different sintering temperature	158
5.72	Comparison of (a) real part of permeability, (b) imaginary part of permeability, and (c) magnetic loss tangent with a frequency of sample $x = 0.3$ at different sintering temperature	158
5.73	Comparison of (a) real part of permeability, (b) imaginary part of permeability, and (c) magnetic loss tangent with frequency of sample $x = 0.4$ at different sintering temperature	158
5.74	Comparison of (a) real part of permeability, (b) imaginary part of permeability, and (c) magnetic loss tangent with frequency of sample $x = 0.5$ at different sintering temperature	158
5.75	Comparison of (a) magnitude of the reflection coefficient, (b) phase of the reflection coefficient, (c) magnitude of the transmission coefficient and (d) phase of the transmission coefficient with frequency of pure BFO sample at different sintering temperatures using the two-port technique	159
5.76	Comparison of (a) magnitude of the reflection coefficient, (b) phase of the reflection coefficient, (c) magnitude of the transmission coefficient and (d) phase of the transmission coefficient with frequency for sample $x = 0.1$ at different sintering temperatures using the two-port technique	160
5.77	Comparison of (a) magnitude of the reflection coefficient, (b) phase of the reflection coefficient, (c) magnitude of the transmission coefficient and (d) phase of the transmission coefficient with frequency for sample $x = 0.2$ at different sintering temperatures using the two-port technique	161
5.78	Comparison of (a) magnitude of the reflection coefficient, (b)	161

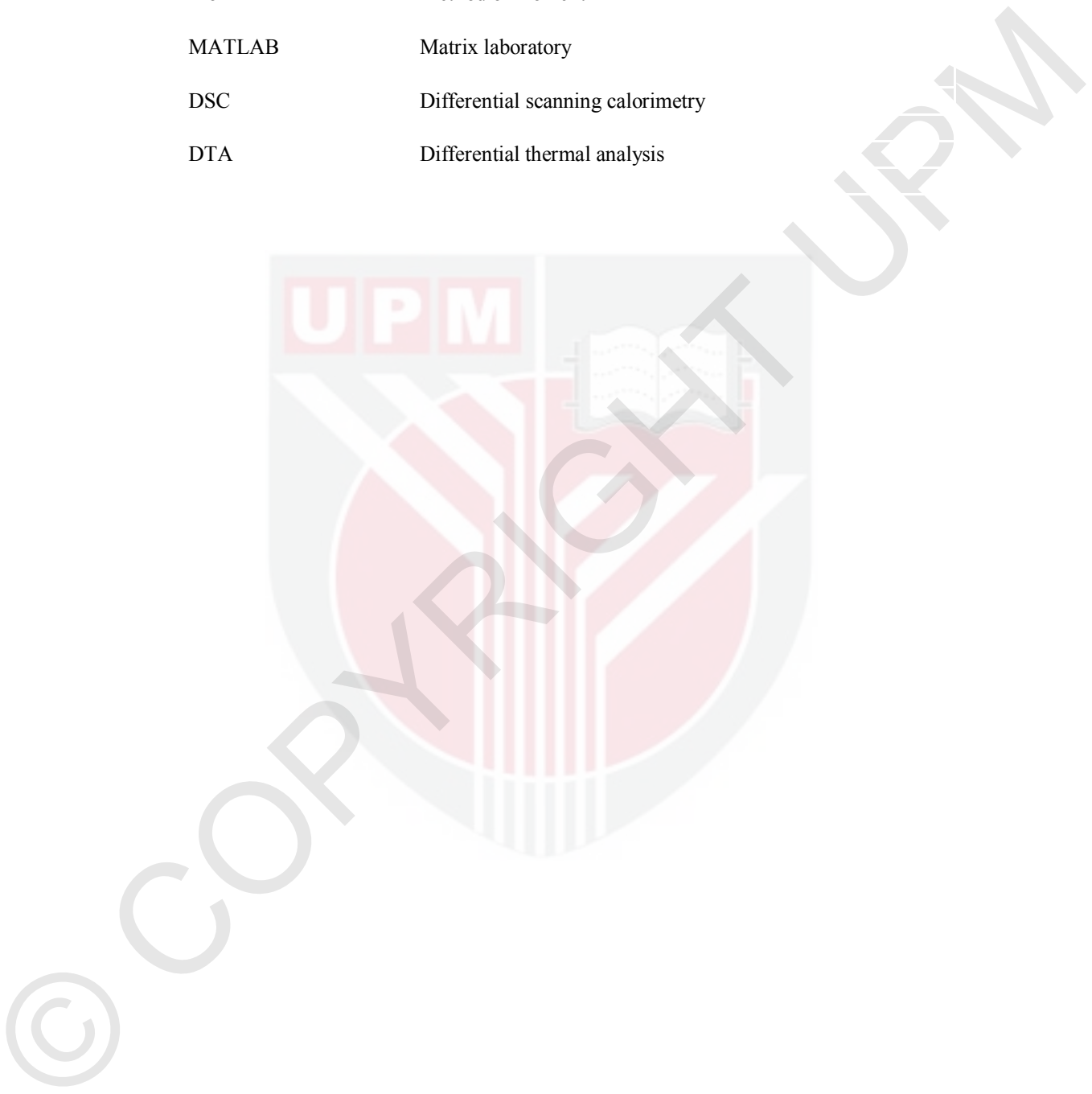
	phase of the reflection coefficient, (c) magnitude of the transmission coefficient and (d) phase of the transmission coefficient with frequency for sample $x = 0.3$ at different sintering temperatures using the two-port technique	
5.79	Comparison of (a) magnitude of the reflection coefficient, (b) phase of the reflection coefficient, (c) magnitude of the transmission coefficient and (d) phase of the transmission coefficient with frequency for sample $x = 0.4$ at different sintering temperatures using the two-port technique	162
5.80	Comparison of (a) magnitude of the reflection coefficient, (b) phase of the reflection coefficient, (c) magnitude of the transmission coefficient and (d) phase of the transmission coefficient with frequency for sample $x = 0.5$ at different sintering temperatures using the two-port technique	162
5.81	Comparison of the magnitude of the reflection coefficient or reflection loss in decibels with frequency of (a) pure BFO (or $x = 0.0$), (b) $x = 0.1$, (c) $x = 0.2$, (d) $x = 0.3$, (e) $x = 0.4$ and (f) $x = 0.5$ at different sintering temperature using the one-port technique	164
5.82	Variation in the magnitude of the reflection coefficient or reflection loss in decibels with frequency of sample $x = 0.0$ with thickness $d = 3$ mm using the one-port technique	165
5.83	Comparison of the magnitude of the reflection coefficient or reflection loss in decibels using the one-port technique measured at the thicknesses of $d = 1$ mm and 3 mm for sample sintered at (a) $600\text{ }^{\circ}\text{C}$, (b) $650\text{ }^{\circ}\text{C}$, and (d) $700\text{ }^{\circ}\text{C}$	168
6.1	Room temperature M - H hysteresis loop of Batch-1 samples	200
6.2	FESEM image and EDX result for sample $x = 0.3$ from Batch-1. Note that this is the repeated sample; the sample is reprepared and the image is remeasured using the FESEM and EDX analysis.	205
6.3	Complex relative permittivity vs. Y-concentration at 10 GHz in each batches of samples: (a) Batch-1, (b) Batch-2 and (c) Batch-3	205
6.4	Complex relative permeability vs. Y-concentration at 10 GHz in each batches of samples: (a) Batch-1, (b) Batch-2 and (c) Batch-3	205
6.5	Complex relative permittivity: (a) dielectric constant, (b) dielectric loss factor, and (c) dielectric loss tangent vs. sintering temperatures at 10 GHz in each samples	206

6.6	Complex relative permeability: (a) dielectric constant, (b) dielectric loss factor, and (c) dielectric loss tangent <i>vs.</i> sintering temperatures at 10 GHz in each samples	206
6.7	Magnitude of the: (a) reflection and (b) transmission coefficient <i>vs.</i> Y-concentration at 10 GHz in each batches of samples	206
6.8	Magnitude of the: (a) reflection and (b) transmission coefficient <i>vs.</i> sintering temperatures at 10 GHz in each samples	207
6.9	Phase diagram of $(1-x)\text{BiFeO}_3-x\text{LaMnO}_3$ ($x = 0.0-1.0$) solid solution	208
6.10	Phase diagram of $\text{BiFeO}_3-\text{BaTiO}_3$ solid solution	208

LIST OF ABBREVIATIONS

ABO ₃	Perovskite structures
BFO or BiFeO ₃	Bismuth ferrites
EM	Electromagnetic
TGA	Thermogravimetric analysis
XRD	X-ray diffraction
FESEM	Field emission scanning electron microscope
EDX	Energy-dispersive X-ray spectroscopy
VSM	Vibrating-sample magnetometer
MNA	Microwave network analyzer
Fe ₃ O ₄	Iron (II,III) Oxide or Ferrosoferric Oxide or Magnetite
Fe ²⁺	Iron(II) ions or ferrous ion
Fe ³⁺	Iron(III) ions or ferric ion
BaTiO ₃	Barium titanate
KNbO ₃	Potassium niobate
K ₂ SeO ₄	Potassium selenate
Cs ₂ CdI ₄	Cesium tetraiodocadamate
BaNiF ₄	Barium tetrafluoronickelate
TM	Transverse magnet
TE	Transverse electric
MUT	Material under test
FEM	Finite element method
NRW	Nicholson-Ross-Weir

FDTD	Finite difference time domain
MoM	Method of moment
MATLAB	Matrix laboratory
DSC	Differential scanning calorimetry
DTA	Differential thermal analysis



LIST OF SYMBOLS

T_C	Curie temperature
T_N	Néel temperature
ω	Angular frequency of a wave (rad/s)
σ	Conductivity (S/m)
χ	Magnetic susceptibility
f	Frequency (Hz)
E	Electric field intensity (V/m)
D	Electric flux density (C/m^2)
J	Electric current density (A/m^2)
H	Magnetic field intensity (A/m)
B	Magnetic flux density (T)
ρ	Electric charge density (C/m^3)
Z_o	Impedance of free space (377Ω)
γ	Complex propagation constant (1/m)
α	Attenuation constant (1/m)
β	Phase constant (rad/m)
μ_o	Permeability of free space, $\mu_o = 1.257 \times 10^{-6} H/m$
ϵ_o	Permittivity of free space, $\epsilon_o = 8.854 \times 10^{-12} F/m$
ϵ_r^*	Complex relative permittivity
μ_r^*	Complex relative permeability
$\tan \delta$	Loss tangent
M_s	Saturation magnetization (emu/g)

M_r	Remnant magnetization (emu/g)
H_c	Coercivity or coercive force or coercive field (Oe)
S-parameters	Scattering-parameters (e.g. S_{11} , S_{21} , S_{12} , S_{22})
RL_{min}	Minimum reflection loss (dB)

CHAPTER 1

INTRODUCTION

1.1 Multiferroics

The term “multiferroic” was first introduced by Hans Schmid in 1994, which describes a class of materials that show simultaneous coexistence of at least two or more ferroic order properties (i.e. ferroelectricity, ferromagnetism, ferroelasticity, ferrotoroidic, ferrimagnetic) in the same material (Eerenstein et al., 2006; Pradhan et al., 2005) (Figure 1). The interaction or coupling between the magnetic and electrical order parameters in the multiferroic materials is called the magnetoelectric (ME) effect (Ding et al., 2011; Wang et al., 2006). On the other hand, the magnetoelectric effect describes the effect of the external magnetic field induces electric polarization or the external electric field induces magnetic moment on the physical properties of crystals (Siratori et al., 1992). From the applications aspect, the magnetoelectric coupling effect could permit data to be written electrically and read magnetically such as ferroelectric random access memory (FeRAM) and magnetic data storage (Mikolajczyk et al., 2008). Multiferroic materials also show great potential in spintronics devices, sensors and transducers. (Li et al., 2007b; Mukherjee et al., 2015; Mukherjee et al., 2012b). Some examples of a material exhibiting multiferroic behavior are TbMnO_3 , LuMnO_3 , LuFe_2O_4 , “PZTFT”, BiFeO_3 and BiMnO_3 (Cheong & Mostovoy, 2007; Evans et al., 2013; Rao et al., 2012). Among these materials, BiFeO_3 has attracted much attention because it has relatively high ferroelectric Curie temperature (T_C) and antiferromagnetic Néel temperature (T_N) at room temperature as compared with other multiferroic materials (Majid et al., 2015).

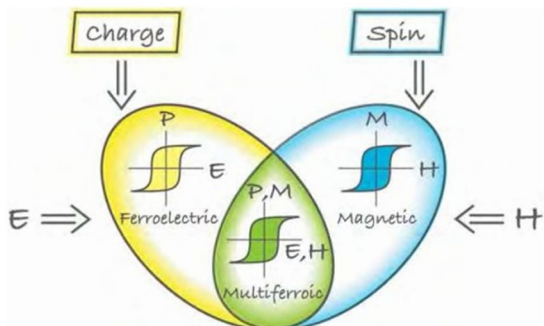


Figure 1: Schematic diagram of multiferroic materials (Areef Billah, 2016)

1.2 Bismuth Ferrite

Bismuth ferrite (BiFeO_3 or BFO) is one of the multiferroic family, that possess the existence of antiferromagnetic and ferroelectric ordering simultaneously at room temperature (Ruelle et al., 2004; Vijayanand et al., 2009). BFO has captured great attention due to its distinctive ability to maintain both electric and magnetic dipole moments at room temperature (Mikolajczyk et al., 2008). BFO has a rhombohedral distorted perovskite structure with space group R3c (Luo et al., 2014). BFO also has an antiferromagnetic Néel temperature, $T_N \sim 370^\circ\text{C}$, and ferroelectric Curie temperature, $T_C \sim 830^\circ\text{C}$ (Miao et al., 2008; Mukherjee et al., 2012b).

1.3 Microwave Absorption as Part of Microwave Studies in BFO

The study of the microwave absorption properties in BFO has captured great attention nowadays due to its applications and benefits. Microwave absorption is dominated by the complex relative permittivity and permeability of a material. The development of smartphone technologies, wireless, or defense for anti-radar coatings (Ramezanzadeh et al., 2017; Rusly et al., 2018; Sharbati and Amiri, 2017) produces radiations and electromagnetic interference (EMI) (Mousavinia et al., 2014; Sharbati and Amiri, 2017). These activities can cause serious problems to human health and disturb the operation of machines (Singh et al., 2018). Thus, it is important to produce a material which can absorb the microwaves energy to protect the humans from electromagnetic hazards known as microwave absorber material (MAM).

Good performance of MAMs can be achieved by controlling several parameters such as the chosen element and amount of doping, thickness of the absorber material, synthesis process, and temperature. Several studies have been reported that BFO can be used as good MAMs (Sun et al., 2020; Mohd Idris et al., 2016). Recently, BFO composites have been expected to exhibit high-efficiency MAMs because of its good magnetic and electric properties. BFO has a special feature combining the G-type antiferromagnetic spin ordering with the $T_N \sim 370^\circ\text{C}$ and ferroelectric properties with the $T_C \sim 830^\circ\text{C}$ simultaneously at room temperature. Furthermore, it exhibits featured frequency response in the microwave fields due to the crystal structure distortion, defects and its magnetoelectric (ME) coupling.

1.4 Problem Statement

Various synthesis method was introduced to synthesize the BFO compound such as the conventional solid-state reaction method, rapid liquid phase sintering method, mechanochemical method, microwave sintering method, and several chemical routes such as wet chemical method, sol-gel method, hydrothermal method, modified Pechini method, auto-combustion method, ferrioxalate precursor method and microwave-assisted method. However, the conventional solid-state reaction method uses high reaction temperatures and produces coarser powder with micro-sized particles (Nalwa & Garg, 2008). In the solid-state reaction (Achenbach et al., 1967; Kumar et al., 2000)

and sol-gel method (Kim et al., 2005), the synthesized BFO powders were leached with nitric acid to eliminate the impurity phases. Most of the chemical routes were chosen to fabricate the BFO nanoparticles. Most of the techniques involve the use of low reaction temperature and produces nano-sized particles. However, they require several parameters such as temperature, pressure, time, solvent, chelating agent and polymerizing agent. Other techniques like the microwave sintering method (Cai et al., 2013) and mechanochemical method (Egorysheva et al., 2013) are laborious and time-consuming. In this study, the thermal treatment method is applied to decrease the sintering temperature of BFO as well as to provide the nano-scale particles of BFO. Moreover, the thermal treatment method provides many advantages such as easy to handle, high flexibility, reproducibility with constant quality, environmentally friendly and capable to amend the chemical structure into desirable properties by controlling its particles sizes as well as the movement of the metallic ions and oxygen atoms during the heating process (Goodarz Naseri et al., 2011b). Synthesis and characterization of $\text{BiFe}_{1-x}\text{Y}_x\text{O}_3$ samples using modified thermal treatment method has been rarely done. Although the mentioned methods enhanced the ferroelectric properties of the BFO system, the magnetic properties remain inferior. Bulk BFO usually has a weak magnetic behavior or low magnetization value (Das et al., 2012; Najm et al., 2016; Suharno et al., 2014; Yan et al., 2013; Yang et al., 2010b) due to residual magnetic moments from canted spin structures (Pradhan et al., 2005) that hinders or limits its practical applications. BFO has a spiral spin structure with an incommensurate spiral period of ~ 62 nm, which prevents the net magnetization and the observation of the linear magnetoelectric effect (Mao et al., 2012). To overcome these problems, researchers have attempted to dope with alkaline earth metal, lanthanide, or rare-earth metal element like Ba, La, Sm, Gd and Y (Nalwa et al., 2008; Singh et al., 2014; Uniyal & Yadav, 2008; Yang et al., 2010a; Yuan et al., 2007) on A-site of BFO, or doping with Cr and Ti (Kumar & Yadav, 2011; Kumar & Yadav, 2007) on B-site of BFO, or co-doping with Gd and Co (Song et al., 2014b), Ba and Gd (Das et al., 2012), Y and Mn (Mukherjee et al., 2014a) and Eu and Mn (Zhu et al., 2017) on A- and B-sites of BFO. Previous works have shown that doping/substitution at Fe-sites could enhance the magnetization of BFO systems (Kumar & Yadav, 2011; Kumar & Yadav, 2007; Najm et al., 2016). The modified thermal treatment method corresponds to a modification technique that has been done to this method such as the use of nitric acid to dissolve the bismuth nitrate salt during the mixing process (Mustapa Zahari et al., 2017). Y^{3+} is a nonmagnetic ion and it was expected to give a possible contribution to the enhancement magnetic properties of BFO due to change in Fe-O-Fe bond angles (Najm et al., 2016). Furthermore, no literature has been found reporting on the microwave properties of $\text{BiFe}_{1-x}\text{Y}_x\text{O}_3$ ceramics at the X-band frequency range and the characteristics of Y-substitution using a modified thermal treatment method are not yet known. Recently, attempts have been made focusing on the absorption properties of BFO at 2-18 GHz in the form of composite (e.g. paraffin composite, epoxy resin composite, wax composite) (Luo et al., 2014; Rusly et al., 2020). However, less info has been reported on the absorption properties of BFO ceramics at room temperature and at 8-12 GHz. In this work, we have reported the structural, magnetic, and microwave properties of $\text{BiFe}_{1-x}\text{Y}_x\text{O}_3$ ceramics at room temperature prepared via a modified thermal treatment method.

1.5 Research Objectives

1. To synthesize $\text{BiFe}_{1-x}\text{Y}_x\text{O}_3$ samples with $x = 0.0, 0.1, 0.2, 0.3, 0.4$, and 0.5 using a modified thermal treatment method.
2. To study the effects of yttrium substitution at the Fe-site of BFO system on the structural and magnetic properties using the XRD, FESEM in conjunction with EDX, and VSM.
3. To study the effects of yttrium substitution on the microwave properties using a closed waveguide technique at the frequency range of 8-12 GHz. Microwaves characterization technique gives information on the reflection, transmission and absorption properties of the samples.
4. To study the effects of different sintering temperatures in $\text{BiFe}_{1-x}\text{Y}_x\text{O}_3$ ($x = 0.0, 0.1, 0.2, 0.3, 0.4$, and 0.5) samples on its structural, magnetic, and microwave properties using the XRD, FESEM, VSM and MNA analysis

1.6 Limitations

Lack of calcined powder to exhibit good magnetic properties in all samples requires the powder to be sintered at 50°C higher than the calcination temperature in each batch of the samples. Calcination and sintering temperatures above 700°C led to the melting of pellets. For electromagnetic studies, there are some limitations in the research work such as the frequency range is limited to the waveguide sensor which operates at only 8-12 GHz following the recommended frequency for rectangular waveguide (TE_{10} , WR90) (Rulf & Robertshaw, 1987), and also the thickness of the measured samples was thin, which was 1 mm.

1.7 Chapter Organization

The whole thesis contains six chapters. The first chapter describes a general introduction of the multiferroics compound and bismuth ferrites as one of the group members in the multiferroic family. The problem statements and research objectives are also stated in this chapter. The second chapter is the literature review section. This chapter reviews the bismuth ferrites as multiferroic material and their electrical and magnetic properties as well as methods to synthesize the bismuth ferrites. This chapter also summarizes the doping or substitution elements at the A-sites, B-sites, and co-doping at A- and B-sites of the bismuth ferrites system. The structural, morphological and magnetic analysis related to bismuth ferrites is reviewed. The previous works related to microwave measurement techniques, their limitations, and several research works related to microwave absorption studies of bismuth ferrites are also reviewed. The third chapter discusses the theory of magnetism which relevant to bismuth ferrites as a magnetic material. The earlier chapter describes the origin of magnetism and the classification of magnetic materials. This chapter also discusses the magnetic hysteresis loop, polarization in dielectrics, mechanism of dielectric polarization, ferroelectric behavior, and mechanism of multiferroic. The wave equation, the calculation of the reflection and transmission coefficient of a three-layered media, the Nicholson-Ross-Weir method to determine the complex permittivity and permeability from S_{11} and S_{21} ,

the half-wavelength effect due to sample thickness effect, and finally the reflection coefficient equation determined by microwave absorption measurement are described in brief at the end of this chapter. The fourth chapter discusses the experimental procedure such as the materials and methods to synthesize the $\text{BiFe}_{1-x}\text{Y}_x\text{O}_3$ samples. The characterization of $\text{BiFe}_{1-x}\text{Y}_x\text{O}_3$ samples using TGA, XRD, FESEM, EDX, VSM and MNA as well as its basic principle is discussed in brief in this chapter. The fifth chapter discusses the formation of BFO nanoparticles using a modified thermal treatment method. The thermal, structural, magnetic, and electromagnetic analysis of $\text{BiFe}_{1-x}\text{Y}_x\text{O}_3$ samples using TGA, XRD, FESEM, EDX, VSM, and MNA are discussed in this chapter. The last chapter of the thesis or the sixth chapter summarizes the conclusions and suggestions or recommendations in future work. This chapter also lists the references and appendices of the research work.



REFERENCES

- Abbas, Z. (2000). *Determination of the dielectric properties of materials at microwave frequencies using rectangular waveguide*. PhD Thesis, University of Leeds, England.
- Abbas, Z., Pollard, R. D., & Kelsall, R. W. (2001). Complex permittivity measurements of Ka-band using rectangular dielectric waveguide. *IEEE Transactions on Instrumentation and Measurement*, 50(5): 1334–1342.
- Achenbach, G. D., James, W. J., & Gerson, R. (1967). Preparation of single-phase polycrystalline BiFeO₃. *Journal of The American Ceramic Society - Discussions and Notes*, 39: 437.
- Ain, R. S. N., Halim, S. A., & Hashim, M. (2012). Effect of Sm-doping on magnetic and dielectric properties of BiFeO₃. *Advanced Materials Research*, 501: 329–333.
- Akhtar, M. N., Hussain, T., Khan, M. A., & Ahmad, M. (2018). Structural, magnetic, dielectric and high frequency response of synthesized rare earth doped bismuth nano garnets (BIG). *Results in Physics*, 10: 784–793.
- Al-Hada, N. M., Saion, E. B., Shaari, A. H., Kamarudin, M. A., Flaifel, M. H., Hj Ahmad, S., & Gene, A. (2014). A facile thermal-treatment route to synthesize the semiconductor CdO nanoparticles and effect of calcination. *Materials Science in Semiconductor Processing*, 26: 460–466.
- Ali, A. (2015). *Effects of MgO, MgB₂ and YBCO addition on formation, microstructure and superconducting properties of Bi_{1.6}Pb_{0.4}Sr₂Cu₂O_δ ceramic*. PhD Thesis, Universiti Putra Malaysia, Malaysia.
- Allaedini, G., Tasirin, S. M., & Aminayi, P. (2015). Magnetic properties of cobalt ferrite synthesized by hydrothermal method. *International Nano Letters*, 5: 183–186.
- Anthonyraj, C., Muneeswaran, M., Gokul Raj, S., Giridharan, N. V., Sivakumar, V., & Senguttuvan, G. (2014). Effect of samarium doping on the structural, optical and magnetic properties of sol-gel processed BiFeO₃ thin films. *Journal of Materials Science: Materials in Electronics*. Doi: 10.1007/s10854-014-2361-9
- Areef Billah, A. H. M. (2016). *Investigation of multiferroic and photocatalytic properties of Li doped BiFeO₃ nanoparticles prepared by ultrasonication*. Master Thesis, Bangladesh University of Engineering and Technology, Bangladesh.
- Asif, M., Nadeem, M., Imran, M., Ahmad, S., Musaddiq, S., Abbas, W., Gilani, Z. A., Sharif, M. K., Warsi, M. F., Khan, M. A. (2019). Structural, magnetic and dielectric properties of Ni-Co doped BiFeO₃ multiferroics synthesized via micro-emulsion route. *Physica B: Condensed Matter*, 552: 11–18.

- Azuma, M., Niitaka, S., Hayashi, N., Oka, K., Tanako, M., Funakubo, H., & Shimakawa, Y. (2008). Rhombohedral–tetragonal phase boundary with high Curie temperature in $(1-x)$ BiCoO_3 – $x\text{BiFeO}_3$ solid solution. *Japanese Journal of Applied Physics*, 47(9): 7579–7581.
- Bakhtiari, S., Ganchev, S. I., & Zoughi, R. (1993). Open-ended rectangular waveguide for nondestructive thickness measurement and variation detection of lossy dielectric slabs backed by a conducting plate. *IEEE Transactions on Instrumentation and Measurement*, 42(1): 19–24.
- Bauer, W., & Westfall, G. D. (2011). *University physics with modern physics (International)*. New York: The McGraw-Hill Companies, Inc.
- Beheshti, K. A., & Yousefi, M. (2020). Impact of Mg-Zr substituted on the magnetic and microwave absorption properties of $\text{BaFe}_{12-2x}\text{Mg}_x\text{Zr}_x\text{O}_{19}$ ($0.25 \leq x \leq 1.5$). *International Journal of Applied Ceramic Technology*, 17(5): 2240–2249.
- Bellakki, M. B., & Manivannan, V. (2010). Citrate-gel synthesis and characterization of yttrium-doped multiferroic BiFeO_3 . *Journal of Sol-Gel Science Technology*, 53: 184–192.
- Bernardo, M. S. (2014). Synthesis, microstructure and properties of BiFeO_3 -based multiferroic materials: A review. *Boletin De La Sociedad Espanola De Ceramica y Vidrio Articulo De Revision*, 53(1): 1–14.
- Bi, S., Li, J., Mei, B., Su, X. J., Ying, C. Z., & Li, P. H. (2018). Effect of Zn doping on the microwave absorption of BFO multiferroic materials. *IOP Conference Series: Materials Science and Engineering*, 292(1): 1–5.
- Biasotto, G., Simoes, A. Z., Foschini, C. R., Zaghet, M. A., Varela, J. A., & Longo, E. (2011). Microwave-hydrothermal synthesis of perovskite bismuth ferrite nanoparticles. *Materials Research Bulletin*, 46: 2543–2547.
- Birkholz, M. (2006). *Thin Film Analysis by X-ray Scattering*. Weinheim: Wiley-VCH.
- Bozgeyik, M. S., Katiyar, R. K., & Katiyar, R. S. (2018). Improved magnetic properties of bismuth ferrite ceramics by La and Gd co-substitution. *Journal of Electroceramics*, 40(3): 247–256.
- Brown W. D., Hess, D., Desai, V., & Jamal Deen, M. (2006, May). *What is a dielectric? An historical perspective*. [Electrochemistry Encyclopedia]. Retrieved from <https://knowledge.electrochem.org/encycl/art-d01-dielectrics.htm>
- Bucci, J. D., Robertson, B. K., & James, W. J. (1972). The precision determination of the lattice parameters and the coefficients of thermal expansion of BiFeO_3 . *Journal of Applied Crystallography*, 5(3): 187–191.
- Cai, D., Li, J., Tong, T., Jin, D., Yu, S., & Cheng, J. (2012). Phase evolution of bismuth ferrites in the process of hydrothermal reaction. *Materials Chemistry and Physics*, 134(1): 139–144.

- Cai, S. (2013). *Bismuth-containing multiferroics; Synthesis, structure and magnetic properties*. Master Thesis, Chalmers University of Technology, Sweden.
- Cai, W., Fu, C., Hu, W., Chen, G., & Deng, X. (2013). Effects of microwave sintering power on microstructure, dielectric, ferroelectric and magnetic properties of bismuth ferrite ceramics. *Journal of Alloys and Compounds*, 554: 64–71.
- Chakraborty, S., Mukherjee, S., & Mukherjee, S. (2013). Effect of yttrium doping on the properties of bismuth ferrite: A review. *International Journal of Semiconductor Science & Technology*, 3(1): 1–10.
- Chanda, U. K. (2013). *Effect of Processing, Dopant and microwave sintering on the dielectric properties of BiFeO₃ ceramic*. Master Thesis, National Institute of Technology Rourkela, India.
- Chang, F., Zhang, N., Yang, F., Wang, S., & Song, G. (2007). Effect of Cr substitution on the structure and electrical properties of BiFeO₃ ceramics. *Journal of Physics D: Applied Physics*, 40(24): 7799–7803.
- Chaodan, Z., Jun, Y., Duanming, Z., Bin, Y., Yunyi, W., Longhai, W., Yunbo, W., & Wenli, Z. (2007). Processing and ferroelectric properties of Ti-doped BiFeO₃ ceramics. *Integrated Ferroelectrics*, 94(1): 31–36.
- Chaudhuri, A., & Mandal, K. (2012). Enhancement of ferromagnetic and dielectric properties of lanthanum doped bismuth ferrite nanostructures. *Materials Research Bulletin*, 47(4): 1057–1061.
- Chaudhuri, A., & Mandal, K. (2014). Study of structural, ferromagnetic and ferroelectric properties of nanostructured barium doped bismuth ferrite. *Journal of Magnetism and Magnetic Materials*, 353: 57–64.
- Chaudhuri, A., Mitra, S., Mandal, M., & Mandal, K. (2010). Nanostructured bismuth ferrites synthesized by solvothermal process. *Journal of Alloys and Compounds*, 491(1–2): 703–706.
- Chen, C., Cheng, J., Yu, S., Che, L., & Meng, Z. (2006). Hydrothermal synthesis of perovskite bismuth ferrite crystallites. *Journal of Crystal Growth*, 291(1): 135–139.
- Chen, X., Wu, Y., Zhang, J., & Chen, X. (2012). Giant magnetic enhancement across a ferroelectric-antiferroelectric phase boundary in Bi_{1-x}Y_xFeO₃. *Science China: Physics, Mechanics and Astronomy*, 55(3): 404–408.
- Chen, X. Z., Qiu, Z. C., Zhou, J. P., Zhu, G., Bian, X. B., & Liu, P. (2011). Large-scale growth and shape evolution of bismuth ferrite particles with a hydrothermal method. *Materials Chemistry and Physics*, 126(3): 560–567.
- Cheng, Z. X., Li, A. H., Wang, X. L., Dou, S. X., Ozawa, K., Kimura, H., Zhang, S., & Shrout, T. R. (2008a). Structure, ferroelectric properties, and magnetic

- properties of the La-doped bismuth ferrite. *Journal of Applied Physics*, 103(07E507): 1–3.
- Cheng, Z. X., Wang, X. L., Kimura, H., Ozawa, K., & Dou, S. X. (2008b). La and Nb codoped BiFeO₃ multiferroic thin films on LaNiO₃/Si and IrO₂/Si substrates. *Applied Physics Letters*, 92(092902): 1–3.
- Cheong, S.-W., & Mostovoy, M. (2007). Multiferroics: a magnetic twist for ferroelectricity. *Nature Materials*, 6: 13–20.
- Cho, C. M., Noh, J. H., Cho, I. S., An, J. S., Hong, K. S., & Kim, J. Y. (2008). Low-temperature hydrothermal synthesis of pure BiFeO₃ nanopowders using triethanolamine and their applications as visible-light photocatalysts. *Journal of the American Ceramic Society*, 91(11): 3753–3755.
- Choi, E.-M., Patnaik, S., Weal, E., Sahonta, S.-L., Wang, H., Bi, Z., Xiong, J., Blamire, M. G., Jia, Q. X., & MacManus-Driscoll, J. L. (2011). Strong room temperature magnetism in highly resistive strained thin films of BiFe_{0.5}Mn_{0.5}O₃. *Applied Physics Letters*, 98(012509): 1–3.
- Chybczynska, K., Lawniczak, P., Hilczer, B., Leska, B., Pankiewicz, R., Pietraszko, A., Kępiński, L., Kałuski, T., Cieluch, P., Matelski, F., & Andrzejewski, B. (2014). Synthesis and properties of bismuth ferrite multiferroic nanoflowers. *Journal of Materials Science*, 49(6): 2596–2604.
- Collin, R. E. (1990). *Field Theory of Guided Waves*. New York: Wiley-IEEE Press.
- Costa, F., Borgese, M., Degiorgi, M., & Monorchio, A. (2017). Electromagnetic characterisation of materials by using transmission/reflection (T/R) devices. *Electronics*, 6(95): 1–27.
- Cullity, B. D. (1978). *Elements of X-ray Diffraction*. Massachusetts: Addison-Wesley.
- Das, R., & Mandal, K. (2011). Effect of barium substitution on ferroelectric and magnetic properties of bismuth ferrite. *IEEE Transactions on Magnetics*, 47(10): 4054–4057.
- Das, R., & Mandal, K. (2012). Magnetic, ferroelectric and magnetoelectric properties of Ba-doped BiFeO₃. *Journal of Magnetism and Magnetic Materials*, 324(11): 1913–1918.
- Das, R., Sarkar, T., & Mandal, K. (2012). Multiferroic properties of Ba²⁺ and Gd³⁺ co-doped bismuth ferrite: magnetic, ferroelectric and impedance spectroscopic analysis. *Journal of Physics D: Applied Physics*, 45(455002): 1–10.
- Das, S. R., Bhattacharya, P., Choudhary, R. N. P., & Katiyar, R. S. (2006). Effect of La substitution on structural and electrical properties of BiFeO₃ thin film. *Journal of Applied Physics*, 99(066107): 1–3.

- Deng, L., & Han, M. (2007). Microwave absorbing performances of multiwalled carbon nanotube composites with negative permeability. *Applied Physics Letters*, 91(023119): 1–3.
- Dhir, G., Uniyal, P., & Verma, N. K. (2014). Effect of particle size on multiferroism of barium-doped bismuth ferrite nanoparticles. *Materials Science in Semiconductor Processing*, 27(1): 611–618.
- Dho, J., Qi, X., Kim, H., MacManus-Driscoll, J. L., & Blamire, M. G. (2006). Large electric polarization and exchange bias in multiferroic BiFeO₃. *Advanced Materials*, 18(11): 1445–1448.
- Ding, Y., Wang, T.-H., Yang, W.-C., Lin, T.-C., Tu, C.-S., Yao, Y.-D., & Wu, K.-T. (2011). Magnetization, magnetoelectric effect, and structure transition in BiFeO₃ and (Bi_{0.95}La_{0.05})FeO₃ multiferroic ceramics. *IEEE Transactions on Magnetics*, 47(3): 513–516.
- Dodrill, B.C. (2000) *Magnetic media measurements with a VSM lake shore cryotonics*. [PDF download]. Retrieved from https://www.lakeshore.com/docs/default-source/product-downloads/application-notes/mag-media-app-note.pdf?sfvrsn=7a9c73a4_1
- Du, Y., Cheng, Z. X., Xue Dou, S., Attard, D. J., & Lin Wang, X. (2011). Fabrication, magnetic, and ferroelectric properties of multiferroic BiFeO₃ hollow nanoparticles. *Journal of Applied Physics*, 109(073903): 1–5.
- Durga Rao, T., & Asthana, S. (2014). Evidence of improved ferroelectric phase stabilization in Nd and Sc co-substituted BiFeO₃. *Journal of Applied Physics*, 116(164102): 1–8.
- Dutta, D. P., Mandal, B. P., Naik, R., Lawes, G., & Tyagi, A. K. (2013). Magnetic, ferroelectric, and magnetocapacitive properties of sonochemically synthesized Sc-doped BiFeO₃ nanoparticles. *Journal of Physical Chemistry C*, 117(5): 2382–2389.
- Ederer, C., & Spaldin, N. A. (2005). Weak ferromagnetism and magnetoelectric coupling in bismuth ferrite. *Physical Review B*, 71(060401(R)): 1–4.
- Ederer, C., & Spaldin, N. A. (2006). Electric-field-switchable magnets: The case of BaNiF₄. *Physical Review B*, 74(020401(R)): 1–4.
- Eerenstein, W., Mathur, N. D., & Scott, J. F. (2006). Multiferroic and magnetoelectric materials. *Nature*, 442(7104): 759–765.
- Eerenstein, W., Morrison, F. D., Sher, F., Prieto, J. L., Attfield, J. P., Scott, J. F., & Mathur, N. D. (2007). Experimental difficulties and artefacts in multiferroic and magnetoelectric thin films of BiFeO₃, Bi_{0.6}Tb_{0.3}La_{0.1}FeO₃ and BiMnO₃. *Philosophical Magazine Letters*, 87(3–4): 249–257.

- Eerenstein, W., Morrison, F., Dho, J., Blamire, M., Scott, J., & Mathur, N. (2005). Comment on “Epitaxial BiFeO₃ multiferroic thin film heterostructures.” *Science*, 307(5713): 1203a.
- Efremov, D. V., Jeroen, V. D. B., & Khomskii, D. I. (2004). Bond-versus site-centred ordering and possible ferroelectricity in manganites. *Nature Materials*, 3: 853–856.
- Egerton, R. F. (2005). *Physical principles of electron microscopy: An introduction to TEM, SEM, and AEM (First Edit)*. New York: Springer.
- Egorysheva, A. V., Volodin, V. D., Ellert, O. G., Efimov, N. N., Skorikov, V. M., Baranchikov, A. E., & Novotortsev, V. M. (2013). Mechanochemical activation of starting oxide mixtures for solid-state synthesis of BiFeO₃. *Inorganic Materials*, 49(3): 303–309.
- Evans, D. M., Schilling, A., Kumar, A., Sanchez, D., Ortega, N., Arredondo, M., Katiyar, R. S., Gregg, J. M., & Scott, J. F. (2013). Magnetic switching of ferroelectric domains at room temperature in multiferroic PZTFT. *Nature Communications*, 4(1534): 1–7.
- Fang, L., Liu, J., Ju, S., Zheng, F., Dong, W., & Shen, M. (2010). Experimental and theoretical evidence of enhanced ferromagnetism in sonochemical synthesized BiFeO₃ nanoparticles. *Applied Physics Letters*, 97(242501): 1–3.
- Feldman, Y., Puzenko, A., & Ryabov, Y. (2006). Dielectric relaxation phenomena in complex materials. *Fractals, Diffusion and Relaxation in Disordered Complex Systems: A Special Volume of Advances in Chemical Physics*, 133: 1–125.
- Feng, B. L., Xue, H., & Xiong, Z. X. (2010). Structure and multiferroic properties of Y-doped BiFeO₃ ceramics. *Chinese Science Bulletin*, 55(4–5): 452–456.
- Feng, Y. B., Qiu, T., & Shen, C. Y. (2007). Absorbing properties and structural design of microwave absorbers based on carbonyl iron and barium ferrite. *Journal of Magnetism and Magnetic Materials*, 318(1–2): 8–13.
- Fennie, C. J., & Rabe, K. M. (2005). Ferroelectric transition in YMnO₃ from first principles. *Physical Review B*, 72(100103(R)): 1–4.
- Feroze, A., Idrees, M., Kim, D. kee, Nadeem, M., Siddiqi, S. A., Shaukat, S. F., Atif, M., & Siddique, M. (2017). Low temperature synthesis and properties of BiFeO₃. *Journal of Electronic Materials*, 46(7): 4582–4589.
- Fiebig, M., Fröhlich, D., Kohn, K., Leute, S., Lottermoser, T., Pavlov, V. V., & Pisarev, R. V. (2000). Determination of the magnetic symmetry of hexagonal manganites by second harmonic generation. *Physical Review Letters*, 84(24): 5620–5623.
- Fiebig, M., Lottermoser, T., Meier, D., & Trassin, M. (2016). The evolution of multiferroics. *Nature Reviews Materials*, 1(16046): 1–14.

- Fischer, P., Polomska, M., Sosnowska, I., & Szymanski, M. (1980). Temperature dependence of the crystal and magnetic structures of BiFeO_3 . *Journal of Physics C: Solid State Physics*, 13(10): 1931–1940.
- Gabbasova, Z. V., Kuz'min, M. D., Zvezdin, A. K., Dubenko, I. S., Murahov, V. A., Rakov, D. N., & Krynetsky, I. B. (1991). $\text{Bi}_{1-x}\text{R}_x\text{FeO}_3$ (R = rare earth): a family of novel magnetoelectrics. *Physics Letters A*, 158: 491–498.
- Gao, F., Yuan, Y., Wang, K. F., Chen, X. Y., Chen, F., Liu, J. M., & Ren, Z. F. (2006). Preparation and photoabsorption characterization BiFeO_3 nanowires. *Applied Physics Letters*, 89(10): 3–6.
- Gautam, A., Uniyal, P., Yadav, K. L., & Rangra, V. S. (2012). Dielectric and magnetic properties of $\text{Bi}_{1-x}\text{Y}_x\text{FeO}_3$ ceramics. *Journal of Physics and Chemistry of Solids*, 73(2): 188–192.
- Ghosh, G., Naskar, M. K., Patra, A., & Chatterjee, M. (2006). Synthesis and characterization of PVP-encapsulated ZnS nanoparticles. *Optical Materials*, 28: 1047–1053.
- Ghosh, S., Dasgupta, S., Sen, A., & Maiti, H. S. (2005a). Low-temperature synthesis of nanosized bismuth ferrite by soft chemical route. *Journal of the American Ceramic Society*, 88(5): 1349–1352.
- Ghosh, S., Dasgupta, S., Sen, A., & Maiti, H. S. (2005b). Low temperature synthesis of bismuth ferrite nanoparticles by a ferrioxalate precursor method. *Materials Research Bulletin*, 40: 2073–2079.
- Glazer, A. M. (1972). The classification of tilted octahedra in perovskites. *Acta Crystallographica*, B28: 3384–3392.
- Godara, S., Sinha, N., Ray, G., & Kumar, B. (2014). Combined structural, electrical, magnetic and optical characterization of bismuth ferrite nanoparticles synthesized by auto-combustion route. *Journal of Asian Ceramic Societies*, 2(4): 1–6.
- Goodarz Naseri, M., Saion, E. B., Abbastabar Ahangar, H., Hashim, M., & Shaari, A. H. (2011a). Synthesis and characterization of manganese ferrite nanoparticles by thermal treatment method. *Journal of Magnetism and Magnetic Materials*, 323: 1745–1749.
- Goodarz Naseri, M., Saion, E. B., Abasstabbar Ahangar, H., & Shaari, A. H. (2013). Fabrication, characterization, and magnetic properties of copper ferrite nanoparticles prepared by a simple, thermal-treatment method. *Materials Research Bulletin*, 48: 1439–1446.
- Goodarz Naseri, M., Saion, E. B., Abbastabar Ahangar, H., Shaari, A. H., & Hashim, M. (2010). Simple synthesis and characterization of cobalt ferrite nanoparticles by a thermal treatment method. *Journal of Nanomaterials*, 2010: 1–8.

- Goodarz Naseri, M., Saion, E. B., Hashim, M., Shaari, A. H., & Abasstabar Ahangar, H. (2011b). Synthesis and characterization of zinc ferrite nanoparticles by a thermal treatment method. *Solid State Communications*, 151: 1031–1035.
- Green, M., & Chen, X. (2019). Recent progress of nanomaterials for microwave absorption. *Journal of Materomics*, 5(4): 503–541.
- Han, J.-T., Huang, Y.-H., Wu, X.-J., Wu, C.-L., Wei, W., Peng, B., Huang, W., & Goodenough, J. B. (2006). Tunable synthesis of bismuth ferrites with various morphologies. *Advanced Materials*, 18: 2145–2148.
- Hasar, U. C. (2009). Non-destructive testing of hardened cement specimens at microwave frequencies using a simple free-space method. *NDT&E International*, 42(6): 550–557.
- Hou, Z. L., Zhou, H. F., Yuan, J., Kang, Y. Q., Yang, H. J., Jin, H. B., & Cao, M. S. (2011). Enhanced ferromagnetism and microwave dielectric properties of $\text{Bi}_{0.95}\text{Y}_{0.05}\text{FeO}_3$ nanocrystals. *Chinese Physics Letters*, 28(3): 3–6.
- Hu, Y., Fei, L., Zhang, Y., Yuan, J., Wang, Y., & Gu, H. (2011). Synthesis of bismuth ferrite nanoparticles via a wet chemical route at low temperature. *Journal of Nanomaterials*, 2011(797639): 1–6.
- Hu, Z., Chen, D., Wang, S., Zhang, N., Qin, L., & Huang, Y. (2017). Facile synthesis of Sm-doped BiFeO_3 nanoparticles for enhanced visible light photocatalytic performance. *Materials Science and Engineering B*, 220: 1–12.
- Huang, F., Lu, X., Lin, W., Wu, X., Kan, Y., & Zhu, J. (2006). Effect of Nd dopant on magnetic and electric properties of BiFeO_3 thin films prepared by metal organic deposition method. *Applied Physics Letters*, 89(24): 3–6.
- Huang, F., Wang, Z., Lu, X., Zhang, J., Min, K., Lin, W., Ti, R., Xu, T., He, J., Yue, C., & Zhu, J. (2013). Peculiar magnetism of BiFeO_3 nanoparticles with size approaching the period of the spiral spin structure. *Scientific Reports*, 3(2907): 1–7.
- Hussain, T., Siddiqi, S. A., Atiq, S., & Awan, M. S. (2013). Induced modifications in the properties of Sr doped BiFeO_3 multiferroics. *Progress in Natural Science: Materials International*, 23(5): 487–492.
- Hyde IV, M. W., & Havrilla, M. J. (2008). A nondestructive technique for determining complex permittivity and permeability of magnetic sheet materials using two flanged rectangular waveguides. *Progress in Electromagnetics Research*, 79: 367–386.
- Ida, N. (1992). *Microwave NDT*. The Netherlands: Kluwer Academic Publishers.
- Ikeda, N., Ohsumi, H., Ohwada, K., Ishii, K., Inami, T., Kakurai, K., Murakami, Y., Yoshii, K., Mori, S., Horibe, Y., & Kitô, H. (2005). Ferroelectricity from iron valence ordering in the charge-frustrated system LuFe_2O_4 . *Nature*, 436: 1136–1138.

- Ishimaru, A. (1991). Electromagnetic wave propagation, radiation, and scattering. New Jersey: Prentice Hall.
- Jacobson, A. J., & Fender, B. E. F. (1975). A neutron diffraction study of the nuclear and magnetic structure of BiFeO_3 . *Journal of Physics C: Solid State Physics*, 8(6): 844–850.
- Jahanbin, T., Hashim, M., Matori, K. A., & Waje, S. B. (2010). Influence of sintering temperature on the structural, magnetic and dielectric properties of $\text{Ni}_{0.8}\text{Zn}_{0.2}\text{Fe}_2\text{O}_4$ synthesized by co-precipitation route. *Journal of Alloys and Compounds*, 503(1): 111–117.
- Jia, C., Onoda, S., Nagaosa, N., & Han, J. H. (2006). Bond electronic polarization induced by spin. *Physical Review B*, 74(224444): 1–8.
- Jiang, H., Morozumi, Y., Kumada, N., Yonesaki, Y., Takei, T., & Kinomura, N. (2008). Hydrothermal synthesis of perovskite-type BiFeO_3 . *Journal of the Ceramic Society of Japan*, 116(7): 837–839.
- Jun, Y. K., & Hong, S. H. (2007). Dielectric and magnetic properties in Co- and Nb-substituted BiFeO_3 ceramics. *Solid State Communications*, 144(7–8): 329–333.
- Kadam, R. H., Karim, A., Kadam, A. B., Gaikwad, A. S., & Shirsath, S. E. (2012). Influence of Cr^{3+} substitution on the electrical and magnetic properties of $\text{Ni}_{0.4}\text{Cu}_{0.4}\text{Zn}_{0.2}\text{Fe}_2\text{O}_4$ nanoparticles. *International Nano Letters*, 2(28): 1–5.
- Kalinin, S. V., Suchomel, M. R., Davies, P. K., & Bonnell, D. A. (2002). Potential and Impedance Imaging of Polycrystalline BiFeO_3 Ceramics. *Journal of the American Ceramic Society*, 85(12): 3011–3017.
- Kang, Y. Q., Cao, M. S., Yuan, J., & Shi, X. L. (2009). Microwave absorption properties of multiferroic BiFeO_3 nanoparticles. *Materials Letters*, 63(15): 1344–1346.
- Kazhugasalamoorthy, S., Jegatheesan, P., Mohandoss, R., Giridharan, N. V., Karthikeyan, B., Joseyphus, R. J., & Dhanuskodi, S. (2010). Investigations on the properties of pure and rare earth modified bismuth ferrite ceramics. *Journal of Alloys and Compounds*, 493(1–2): 569–572.
- Khan, A. H., Atiq, S., Anwar Sabieh, M., Naseem, S., & Abbas, S. K. (2018). Optimization of magnetodielectric coupling in Mn substituted BiFeO_3 for potential memory devices. *Journal of Materials Science: Materials in Electronics*. Doi: <https://doi.org/10.1007/s10854-018-9281-z>
- Kharkovsky, S., & Zoughi, R. (2007). Microwave and millimeter wave nondestructive testing: A succinct introduction. *IEEE Instrumentation & Measurement Magazine*, 10: 26–38.

- Khomchenko, V. A., Kiselev, D. A., Vieira, J. M., Jian, L., Kholkin, A. L., Lopes, A. M. L., Pogorelov, Y. G., Araujo, J. P., & Maglione, M. (2008a). Effect of diamagnetic Ca, Sr, Pb, and Ba substitution on the crystal structure and multiferroic properties of the BiFeO_3 perovskite. *Journal of Applied Physics*, 103(024105): 1–6.
- Khomchenko, V. A., Kopcewicz, M., Lopes, A. M. L., Pogorelov, Y. G., Araujo, J. P., Vieira, J. M., & Kholkin, A. L. (2008b). Intrinsic nature of the magnetization enhancement in heterovalently doped $\text{Bi}_{1-x}\text{A}_x\text{FeO}_3$ ($\text{A} = \text{Ca}, \text{Sr}, \text{Pb}, \text{Ba}$) multiferroics. *Journal of Physics D: Applied Physics*, 41(102003): 1–4.
- Kim, J. K., Kim, S. S., Kim, W.-J., & Bhalla, A. S. (2007). Substitution effects on the ferroelectric properties of BiFeO_3 thin films prepared by chemical solution deposition. *Journal of Applied Physics*, 101(014108): 1–3.
- Kim, J. K., Kim, S. S., & Kim, W. J. (2005). Sol-gel synthesis and properties of multiferroic BiFeO_3 . *Materials Letters*, 59(29–30): 4006–4009.
- Kimura, T., Goto, T., Shintani, H., Ishizaka, K., Arima, T., & Tokura, Y. (2003). Magnetic control of ferroelectric polarization. *Nature*, 426: 55–58.
- Kingery, W. D., Bowen, H. K., & Uhlmann, D. R. (1976). *Introduction to Ceramics*. New York: John Wiley & Sons, Inc.
- Koebel, M. M., Jones, L. C., & Somorjai, G. A. (2008). Preparation of size-tunable, highly monodisperse PVP-protected Pt-nanoparticles by seed-mediated growth. *Journal of Nanoparticle Research*, 10: 1063–1069.
- Kong, I., Hj Ahmad, S., Hj Abdullah, M., Hui, D., Nazlim Yusoff, A., & Puryanti, D. (2010). Magnetic and microwave absorbing properties of magnetite-thermoplastic natural rubber nanocomposites. *Journal of Magnetism and Magnetic Materials*, 322(21): 3401–3409.
- Kum-onsa, P., Chanlek, N., Thongbai, P., & Srepusharawoot, P. (2020). Effect of complex defects on the origin of giant dielectric properties of Mg^{2+} -doped BiFeO_3 ceramics prepared by a precipitation method. *Ceramics International*, 46(16): 25017–25023.
- Kumar, A., & Yadav, K. L. (2011). Magnetic, magnetocapacitance and dielectric properties of Cr doped bismuth ferrite nanoceramics. *Materials Science and Engineering B*, 176(3): 227–230.
- Kumar, M. M., Palkar, V. R., Srinivas, K., & Suryanarayana, S. V. (2000). Ferroelectricity in a pure BiFeO_3 ceramic. *Applied Physics Letters*, 76(19): 2764–2766.
- Kumar, M., & Yadav, K. L. (2006). Study of room temperature magnetoelectric coupling in Ti substituted bismuth ferrite system. *Journal of Applied Physics*, 100(7): 1–5.

- Kumar, M., & Yadav, K. L. (2007). Magnetic field induced phase transition in multiferroic $\text{BiFe}_{1-x}\text{Ti}_x\text{O}_3$ ceramics prepared by rapid liquid phase sintering. *Applied Physics Letters*, 91(112911): 1–3.
- Kumar, M., Yadav, K. L., & Varma, G. D. (2008). Large magnetization and weak polarization in sol-gel derived BiFeO_3 ceramics. *Materials Letters*, 62(8–9): 1159–1161.
- Layek, S., & Verma, H. C. (2012). Magnetic and dielectric properties of multiferroic BiFeO_3 nanoparticles synthesized by a novel citrate combustion method. *Advanced Materials Letters*, 3(6): 533–538.
- Lazenga, V. V., Zhang, G., Vanacken, J., Makoed, I. I., Ravinski, A. F., & Moshchalkov, V. V. (2012). Structural transformation and magnetoelectric behaviour in $\text{Bi}_{1-x}\text{Gd}_x\text{FeO}_3$ multiferroics. *Journal of Physics D: Applied Physics*, 45(125002): 1–7.
- Lee, W. E., & Rainforth, W. M. (1994). *Ceramic microstructures: Property control by processing*. London: Chapman & Hall.
- Lee, Y., Wu, J., Chueh, Y., & Chou, L. (2005). Low-temperature growth and interface characterization of BiFeO_3 thin films with reduced leakage current. *Applied Physics Letters*, 87(172901): 1–4.
- Li, J. B., Rao, G. H., Liang, J. K., Liu, Y. H., Luo, J., & Chen, J. R. (2007a). Magnetic properties of $\text{Bi}(\text{Fe}_{1-x}\text{Cr}_x)\text{O}_3$ synthesized by a combustion method. *Applied Physics Letters*, 90(162513): 1–3.
- Li, J., Duan, Y., He, H., & Song, D. (2001). Crystal structure, electronic structure, and magnetic properties of bismuth-strontium ferrites. *Journal of Alloys and Compounds*, 315(1–2): 259–264.
- Li, Jinsong, Lu, W., Suhr, J., Chen, H., Xiao, J. Q., & Chou, T. W. (2017). Superb electromagnetic wave-absorbing composites based on large-scale graphene and carbon nanotube films. *Scientific Reports*, 7(2349): 1–10.
- Li, M., Ning, M., Ma, Y., Wu, Q., & Ong, C. K. (2007b). Room temperature ferroelectric, ferromagnetic and magnetoelectric properties of Ba-doped BiFeO_3 thin films. *Journal of Physics D: Applied Physics*, 40(6): 1603–1607.
- Li, Y., Cao, M.-S., Wang, D.-W., & Yuan, J. (2015a). High-efficiency and dynamic stable electromagnetic wave attenuation for La doped bismuth ferrite at elevated temperature and gigahertz frequency. *Royal Society of Chemistry Advances*, 5(94): 77184–77191.
- Li, Y., Cao, W. Q., Yuan, J., Wang, D. W., & Cao, M. S. (2015b). Nd doping of bismuth ferrite to tune electromagnetic properties and increase microwave absorption by magnetic-dielectric synergy. *Journal of Materials Chemistry C*, 3(36): 9276–9282.

- Li, Y., Fang, X., & Cao, M. (2016a). Thermal frequency shift and tunable microwave absorption in BiFeO₃ family. *Scientific Reports*, 6(24837): 1–6.
- Li, Z.-J., Hou, Z.-L., Song, W.-L., Liu, X.-Da, Wang, D.-W., Tang, J., & Shao, X.-H. (2016b). Mg-substitution for promoting magnetic and ferroelectric properties of BiFeO₃ multiferroic nanoparticles. *Materials Letters*, 175: 207–211.
- Lilienblum, M., Lottermoser, T., Manz, S., Selbach, S. M., Cano, A., & Fiebig, M. (2015). Ferroelectricity in the multiferroic hexagonal manganites. *Nature Physics*, 11: 1–5.
- Liu, S., Luo, H., Yan, S., Yao, L., He, J., Li, Y., He, L., Huang, S., & Deng, L. (2017). Effect of Nd-doping on structure and microwave electromagnetic properties of BiFeO₃. *Journal of Magnetism and Magnetic Materials*, 426: 267–272.
- Liu, Y., Drew, M. G. B., Li, H., & Liu, Y. (2020). An experimental and theoretical investigation into methods concerned with “reflection loss” for microwave absorbing materials. *Materials Chemistry and Physics*, 243(122624): 1–17.
- Luo, L., Wei, W., Yuan, X., Shen, K., Xu, M., & Xu, Q. (2012). Multiferroic properties of Y-doped BiFeO₃. *Journal of Alloys and Compounds*, 540: 36–38.
- Luo, M., Zhou, P. H., Liu, Y. F., Wang, X., & Xie, J. L. (2014). Influence of Y-doping on structure, microwave dielectric and magnetic behaviors in BiFeO₃. *Physica B: Condensed Matter*, 450: 1–6.
- Majid, F., Mirza, S. T., Riaz, S., & Naseem, S. (2015). Sol-Gel Synthesis of BiFeO₃ Nanoparticles. *Materials Today: Proceedings*, 2(10): 5293–5297.
- Mao, W., Li, X., Li, Y., Li, P., Bao, G., Yang, T., & Yang, J. (2012). Structural and magnetic properties of single-phase Bi_{0.9}Eu_{0.1}Fe_{0.95}Co_{0.05}O₃ and Bi_{0.9}Eu_{0.05}La_{0.05}Fe_{0.95}Co_{0.05}O₃ nanoparticles. *Materials Letters*, 76: 135–137.
- Matin, M. A., Hossain, M. N., Ali, M. A., Hakim, M. A., & Islam, M. F. (2019). Enhanced dielectric properties of prospective Bi_{0.85}Gd_{0.15}Fe_{1-x}Cr_xO₃ multiferroics. *Results in Physics*, 12: 1653–1659.
- Mazumder, R., Sujatha Devi, P., Bhattacharya, D., Choudhury, P., Sen, A., & Raja, M. (2007). Ferromagnetism in nanoscale BiFeO₃. *Applied Physics Letters*, 91(062510): 1–3.
- Meredith, R. (1998). *Engineers' handbook of industrial microwave heating*. London: The Institution of Electrical Engineers.
- Miao, H., Zhang, Q., Tan, G., & Zhu, G. (2008). Co-precipitation/hydrothermal synthesis of BiFeO₃ powder. *Journal Wuhan University of Technology, Materials Science Edition*, 23(4): 507–509.
- Mikolajczyk, B., Bedzyk, M., Klug, J., & Lin, J.-C. (2008). X-ray characterization of a multiferroic bismuth ferrite thin film. *Nanoscape*, 5(1): 95–105.

- Mishra, R. K., Pradhan, D. K., Choudhary, R. N. P., & Banerjee, A. (2008). Effect of yttrium on improvement of dielectric properties and magnetic switching behavior in BiFeO_3 . *Journal of Physics: Condensed Matter*, 20(045218): 1–6.
- Mohamed, N. (2017). *Effects of Pr_6O_{11} addition and sintering temperature on structural, optical and luminescence properties of Zn_2SiO_4 based glass ceramic*. PhD Thesis, Universiti Putra Malaysia, Malaysia.
- Mohd Idris, F., Hashim, M., Abbas, Z., Ismail, I., Nazlan, R., & Ibrahim, I. R. (2016). Recent developments of smart electromagnetic absorbers based polymer-composites at gigahertz frequencies. *Journal of Magnetism and Magnetic Materials*, 405: 197–208.
- Mohd Tarmizi, E. Z. (2006). *Optical and electrical properties of transition metal calcium phosphate glasses*. Master Thesis, Universiti Putra Malaysia, Malaysia.
- Mohomed, K. (2016, January 3). *Thermogravimetric analysis (TGA) theory and applications TA instruments-waters LLC*. [PDF download]. Retrieved from <https://www.researchgate.net/file.PostFileLoader.html?id=5876b5fbcb5c2fe1c4be189&assetKey=AS%3A449492081221632%401484178671185>
- Mousavinia, M., Ghasemi, A., & Paimozd, E. (2014). Structural, magnetic, and reflection loss characteristics of Ni/Co/Sn-substituted strontium ferrite/functionalized MWCNT nanocomposites. *Journal of Electronic Materials*, 1–11. Doi: 10.1007/s11664-014-3120-7
- Mukherjee, A., Banerjee, M., Basu, S., Nguyen Thi, K. T., Green, L. A. W., & Pal, M. (2014a). Enhanced magnetic and electrical properties of Y and Mn co-doped BiFeO_3 nanoparticles. *Physica B*, 448: 199–203.
- Mukherjee, A., Basu, S., Manna, P. K., Yusuf, S. M., & Pal, M. (2014b). Giant magnetodielectric and enhanced multiferroic properties of Sm doped bismuth ferrite nanoparticles. *Journal of Materials Chemistry C*, 2(29): 5885–5891.
- Mukherjee, A., Basu, S., Chakraborty, G., & Pal, M. (2012a). Effect of Y-doping on the electrical transport properties of nanocrystalline BiFeO_3 . *Journal of Applied Physics*, 112(014321): 1–8.
- Mukherjee, A., Hossain, S. M., Pal, M., & Basu, S. (2012b). Effect of Y-doping on optical properties of multiferroics BiFeO_3 nanoparticles. *Applied Nanoscience*, 2(3): 305–310.
- Mukherjee, S., Chakraborty, S., & Mukherjee, S. (2012c). A comparative study of pure and rare earth transition metal doped bismuth ferrite. *International Journal of Current Engineering and Technology*, 2(4): 403–408.
- Mukherjee, A., Basu, S., Green, L. A. W., Thanh, N. T. K., & Pal, M. (2015). Enhanced multiferroic properties of Y and Mn codoped multiferroic BiFeO_3 nanoparticles. *Journal of Materials Science*, 50(4): 1891–1900.

- Musa, M. A., Azis, R. S., Osman, N. H., Hassan, J., & Zangina, T. (2017). Structural and magnetic properties of yttrium iron garnet (YIG) and yttrium aluminum iron garnet (YAlG) nanoferrite via sol-gel synthesis. *Results in Physics*, 7: 1135–1142.
- Mustapa Zahari, R., Shaari, A. H., Abbas, Z., Baqiah, H., Chen, S. K., Lim, K. P., & Awang Kechik, M. M. (2017). Simple preparation and characterization of bismuth ferrites nanoparticles by thermal treatment method. *Journal of Materials Science: Materials in Electronics*, 28(23): 17932–17938.
- Mustapa Zahari, R. (2013). *Critical analysis of rectangular waveguide for determination of moisture content in hevea rubber latex*. Master Thesis, Universiti Putra Malaysia, Malaysia.
- Nabiyouni, G., Halakouie, H., & Ghanbari, D. (2017). Microwave synthesis of different morphologies of lead ferrite nanostructures and investigation of magnetic properties. *Journal of Nanostructures*, 7(1): 77–81.
- Naganuma, H., Shimura, N., Miura, J., Shima, H., Yasui, S., Nishida, K., Katoda, T., Iijima, T., Funakubo, H., & Okamura, S. (2008). Enhancement of ferroelectric and magnetic properties in BiFeO₃ films by small amount of cobalt addition. *Journal of Applied Physics*, 103(07E314): 1–3.
- Naik, V. B., & Mahendiran, R. (2009). Magnetic and magnetoelectric studies in pure and cation doped BiFeO₃. *Solid State Communications*, 149(19–20): 754–758.
- Najm, A. A. A., Baqiah, H., Shaari, A. H., Awang Kechik, M. M., Chen, S. K., Mustapa Zahari, R., & Li, Q. (2021). Investigation of structural, dielectric, impedance and magnetic properties of BiFe_{1-x}In_xO₃ (0.0 ≤ x ≤ 0.6) ceramics. *Results in Physics*, 28(104550): 1–7.
- Najm, A. A. A., Shaari, A. H., Baqiah, H., Bin Saion, E., Pah, L. K., Kien, C. S., & Kechik, M. M. A. (2016). Structural, electrical and magnetic properties of BiFe_{1-x}Y_xO₃ (0 ≤ x ≤ 0.6) ceramics. *Journal of Ceramic Science and Technology*, 7(4): 329–334.
- Nalwa, K. S., Garg, A., & Upadhyaya, A. (2008). Effect of samarium doping on the properties of solid-state synthesized multiferroic bismuth ferrite. *Materials Letters*, 62: 878–881.
- Nalwa, K. S., & Garg, A. (2008). Phase evolution, magnetic and electrical properties in Sm-doped bismuth ferrite. *Journal of Applied Physics*, 103(044101): 1–6.
- Naughton, B. T., Majewski, P., & Clarke, D. R. (2007). Magnetic properties of nickel-zinc ferrite toroids prepared from nanoparticles. *Journal of the American Ceramic Society*, 90(11): 3547–3553.
- Navrotsky, A. (1998). Energetics and crystal chemical systematic among ilmenite, lithium niobate, and perovskite structures. *Chemistry of Materials*, 10(10): 2787–2793.

- Newnham, R. E., Kramer, J. J., Schulze, W. A., & Cross, L. E. (1978). Magnetoferroelectricity in Cr_2BeO_4 . *Journal of Applied Physics*, 49(12): 6088–6091.
- Nicolson, A. M., & Ross, G. F. (1970). Measurement of the intrinsic properties of materials by time-domain techniques. *IEEE Transactions on Instrumentation and Measurement*, 19(4): 377–382.
- Pandey, D., & Singh, A. (2009). Structure, synthesis and multiferroic nature of BiFeO_3 and $0.9\text{BiFeO}_3\text{-}0.1\text{BaTiO}_3$: An overview. *Bulletin of Materials Science*, 32(3): 361–367.
- Park, T., Papaefthymiou, G. C., Viescas, A. J., Moodenbaugh, A. R., & Wong, S. S. (2007). Size-dependent magnetic properties of nanoparticles. *Nano Letters*, 7(3): 766–772.
- Popov, Y. F., Zvezdin, A. K., Vorob'ev, G. P., Kadomtseva, A. M., Murashev, V. A., & Rakov, D. N. (1993). Linear magnetoelectric effect and phase transitions in bismuth ferrite, BiFeO_3 . *JETP Letters*, 57(1): 69–73.
- Pozar, D. M. (2005). *Microwave engineering*. Hoboken: John Wiley & Sons, Inc.
- Pradhan, A. K., Zhang, K., Hunter, D., Dadson, J. B., Loutts, G. B., Bhattacharya, P., Katiyar, R., Zhang, J., Sellmyer, D. J., Roy, U. N., Cui, Y., & Burger, A. (2005). Magnetic and electrical properties of single-phase multiferroic BiFeO_3 . *Journal of Applied Physics*, 97(093903): 1–3.
- Puhan, A., Bhushan, B., Kumar, V., Panda, H. S., & Rout, D. (2018). Structural and dielectric properties of Ba, Cr co-doped BiFeO_3 multiferroic nanoparticles. In AIP Conference Proceedings (Vol. 1953).
- Qi, X., Dho, J., Tomov, R., Blamire, M. G., & MacManus-Driscoll, J. L. (2005). Greatly reduced leakage current and conduction mechanism in aliovalent-ion-doped BiFeO_3 . *Applied Physics Letters*, 86(6): 1–3.
- Qian, F. Z., Jiang, J. S., Jiang, D. M., Wang, C. M., & Zhang, W. G. (2010). Improved multiferroic properties and a novel magnetic behavior of Bi $0.8\text{La}_{0.2}\text{Fe}_{1-x}\text{Co}_x\text{O}_3$ nanoparticles. *Journal of Magnetism and Magnetic Materials*, 322(20): 3127–3130.
- Ramesh, R., & Spaldin, N. A. (2007). Multiferroics: Progress and prospects in thin films. *Nature Materials*, 6: 21–29.
- Ramezanzaeh, G., Ghasemi, A., Mozaffarinia, R., & Alizadeh, A. (2017). Electromagnetic wave reflection loss and magnetic properties of M-type $\text{SrFe}_{12-x}(\text{Mn}_{0.5}\text{Sn}_{0.5})_x\text{O}_{19}$ hexagonal ferrite nanoparticles in the Ku microwave band. *Ceramics International*, 43(13): 10231–10238.
- Rao, C. N. R., Sundaresan, A., & Saha, R. (2012). Multiferroic and magnetoelectric oxides: The emerging scenario. *Journal of Physical Chemistry Letters*, 3(16): 2237–2246.

- Ray, J., Biswal, A. K., Acharya, S., Babu, P. D., Siruguri, V., & Vishwakarma, P. N. (2013). Neutron diffraction studies on cobalt substituted BiFeO_3 . *AIP Conference Proceedings*, 1512: 1124–1125.
- Reddy, V. R., Kothari, D., Gupta, A., & Gupta, S. M. (2009). Study of weak ferromagnetism in polycrystalline multiferroic Eu doped bismuth ferrite. *Applied Physics Letters*, 94(8): 2007–2010.
- Rodziah, N., Hashim, M., Idza, I. R., Ismayadi, I., Hapishah, A. N., & Khamirul, M. A. (2012). Applied surface science dependence of developing magnetic hysteresis characteristics on stages of evolving microstructure in polycrystalline yttrium iron garnet. *Applied Surface Science*, 258(7): 2679–2685.
- Rohde, & Schwarz. (2006). *Measurement of dielectric material properties application note*. Asia/Pacific.
- Roosen, A. R., & Craig Carter, W. (1998). Simulations of microstructural evolution: anisotropic growth and coarsening. *Physica A*, 261: 232–247.
- Rout, J., Choudhary, R. N. P., Sharma, H. B., & Shannigrahi, S. R. (2015). Effect of co-substitutions (Ca-Mn) on structural, electrical and magnetic characteristics of bismuth ferrite. *Ceramics International*, 41(7): 9078–9087.
- Rubi, D., Marlasca, F. G., Reinoso, M., Bonville, P., & Levy, P. (2012). Magnetism and electrode dependant resistive switching in Ca-doped ceramic bismuth ferrite. *Materials Science and Engineering B: Solid-State Materials for Advanced Technology*, 177(6): 471–475.
- Ruette, B., Zvyagin, S., Pyatakov, A. P., Bush, A., Li, J. F., Belotelov, V. I., Zvezdin, A. K., & Viehland, D. (2004). Magnetic-field-induced phase transition in BiFeO_3 observed by high-field electron spin resonance: Cycloidal to homogeneous spin order. *Physical Review B*, 69(064114): 1–7.
- Rulf, B., & Robertshaw, G. A. (1987). *Understanding Antennas for Radar, Communications, and Avionics*. New York: Van Nostrand Reinhold.
- Rusly, S. N. A. (2013). *Microstructural, magnetic and dielectric properties of $\text{Bi}_{1-x}\text{Sm}_x\text{FeO}_3$ multiferroic materials*. Master Thesis, Universiti Putra Malaysia, Malaysia.
- Rusly, S. N. A., Ismail, I., Matori, K. A., Abbas, Z., Shaari, A. H., Awang, Z., Ibrahim, I. R., Mohd Idris, F., Mohd Zaid, M. H., Mahmood, M. K. A., & Hasan, I. H. (2020). Influence of different BFO filler content on microwave absorption performances in BiFeO_3 /epoxy resin composites. *Ceramics International*, 46: 737–746.
- Rusly, S. N. A., Matori, K. A., Ismail, I., Abbas, Z., Awang, Z., Idris, F. M., & Ibrahim, I. R. (2018). Effects of crystalline phase formation of multiferroic BiFeO_3 on microwave absorption characteristics. *Journal of Materials Science: Materials in Electronics*, 29(15): 13229–13240.

- Sadiku, M. N. O. (2007). *Elements of Electromagnetics*. New York: Oxford University Press, Inc.
- Saeed, K., Shafique, M. F., Byrne, M. B., & Hunter, I. C. (2012). Planar microwave sensors for complex permittivity characterization of materials and their applications. *Applied Measurement Systems*, 319–350.
- Sakar, M., Balakumar, S., Saravanan, P., & Jaisankar, S. N. (2013). Annealing temperature mediated physical properties of bismuth ferrite (BiFeO_3) nanostructures synthesized by a novel wet chemical method. *Materials Research Bulletin*, 48(8): 2878–2885.
- Sánchez, R. D., Rivas, J., Vaqueiro, P., López-Quintela, M. A., & Caeiro, D. (2002). Particle size effects on magnetic properties of yttrium iron garnets prepared by a sol-gel method. *Journal of Magnetism and Magnetic Materials*, 247: 92–98.
- Selbach, S. M., Tybell, T., Einarsrud, M.-A., & Grande, T. (2007). Size-dependent properties of multiferroic BiFeO_3 nanoparticles. *Chemistry of Materials*, 19(26): 6478–6484.
- Shannon, R. D. (1976). Revised effective ionic radii and systematic studies of interatomic distances in halides and chalcogenides. *Acta Crystallographica A*, 32: 751–767.
- Shao, H., Huang, Y., Lee, H., Suh, Y. J., & Kim, C. O. (2006). Effect of PVP on the morphology of cobalt nanoparticles prepared by thermal decomposition of cobalt acetate. *Current Applied Physics 6SI*: e195–e197.
- Sharbati, A., & Amiri, G. R. (2017). Magnetic, microwave absorption and structural properties of Mg-Ti added Ca-M hexaferrite nanoparticles. *Journal of Materials Science: Materials in Electronics*, 1–5. Doi: 10.1007/s10854-017-8013-0
- Sharma, N., Kumar, S., Mall, A. K., Gupta, R., & Garg, A. (2017). Sr and Mn Co-doped sol-gel derived BiFeO_3 ceramics with enhanced magnetism and reduced leakage current. *Materials Research Express*, 4(015702): 1–9.
- Sharma, P., Kumar, A., & Varshney, D. (2015). Rare earth (La) and metal ion (Pb) substitution induced structural and multiferroic properties of bismuth ferrite. *Journal of Advanced Ceramics*, 4(4): 292–299.
- Shen, H., Xu, J., Wu, A., Zhao, J., & Shi, M. (2009). Magnetic and thermal properties of perovskite YFeO_3 single crystals. *Materials Science and Engineering B*, 157: 77–80.
- Simões, A. Z., Riccardi, C. S., Santos, M. L. Dos, González Garcia, F., Longo, E., & Varela, J. A. (2009). Effect of annealing atmosphere on phase formation and electrical characteristics of bismuth ferrite thin films. *Materials Research Bulletin*, 44: 1747–1752.

- Singh, A. K., Shishkin, A., Koppel, T., & Gupta, N. (2018). A review of porous lightweight composite materials for electromagnetic interference shielding. *Composites Part B: Engineering*, 149: 188–197.
- Singh, S. K., & Ishiwara, H. (2006). Doping Effect of Rare-Earth Ions on Electrical Properties of BiFeO_3 Thin Films Fabricated by Chemical Solution Deposition. *Japanese Journal of Applied Physics*, 45(4B): 3194–3197.
- Singh, V., Sharma, S., Jha, P. K., Kumar, M., & Dwivedi, R. K. (2014). Effect of Y^{3+} substitution on structural, electrical and optical properties of BiFeO_3 ceramics. *Ceramics International*, 40(1 Part B): 1971–1977.
- Siratori, K., Kohn, K., & Kita, E. (1992). Magnetoelectric effect in magnetic materials. *Acta Physica Polonica A*, 81(4–5): 431–465.
- Soegijono, B., Suharno, Hidayati, R., & Suastiyanti, D. (2015). Enhanced microwave absorption properties of Y doped BiFeO_3 . *Asian Journal of Applied Sciences*, 3(4): 555–561.
- Soleimani, H. (2009). *Preparation of $\text{Y}_3\text{Fe}_5\text{O}_{12}$ and $\text{La}_3\text{Fe}_5\text{O}_{12}$ filled PVDF-polymer nanocomposite and their electromagnetic characterisation using FEM simulation rectangular waveguide and NRW method*. PhD Thesis, Universiti Putra Malaysia, Malaysia.
- Song, G. L., Ma, G. J., Su, J., Wang, T. X., Yang, H. Y., & Chang, F. G. (2014a). Effect of Ho^{3+} doping on the electric, dielectric, ferromagnetic properties and T_C of BiFeO_3 ceramics. *Ceramics International*, 40(2): 3579–3587.
- Song, G. L., Su, J., Ma, G. J., Wang, T. X., Yang, H. G., & Chang, F. G. (2014b). Effects of trivalent gadolinium and cobalt co-substitution on the crystal structure, electronic transport, and ferromagnetic properties of bismuth ferrite. *Materials Science in Semiconductor Processing*, 27: 899–908.
- Song, G. L., Zhang, H. X., Wang, T. X., Yang, H. G., & Chang, F. G. (2012). Effect of Sm, Co codoping on the dielectric and magnetoelectric properties of BiFeO_3 polycrystalline ceramics. *Journal of Magnetism and Magnetic Materials*, 324(13): 2121–2126.
- Sözeri, H., Mehmedi, Z., Erdemi, H., Baykal, A., Topal, U., & Aktaş, B. (2016). Microwave properties of $\text{BaFe}_{11}\text{Mg}^{2+}_{0.25}\text{X}^{2+}_{0.25}\text{Ti}^{4+}_{0.25}\text{O}_{19}$ ($\text{X}^{2+} = \text{Cu}, \text{Mn}, \text{Zn}, \text{Ni}$ and Co) nanoparticles in 0–26.5 GHz range. *Ceramics International*, 42(2): 2611–2625.
- Sosnowska, I., Neumaier, T. P., & Steichele, E. (1982). Spiral magnetic ordering in bismuth ferrite. *Journal of Physics C: Solid State Physics*, 15(23): 4835–4846.
- Sosnowska, I., Schäfer, W., Kockelmann, W., Andersen, K. H., & Troyanchuk, I. O. (2002). Crystal structure and spiral magnetic ordering of BiFeO_3 doped with manganese. *Applied Physics A Materials Science & Processing*, 74: 1040–1042.

- Spaldin, N. A. (2011). *Magnetic materials: Fundamentals and applications*. Cambridge: Cambridge University Press.
- Stojadinović, B., Dohčević-Mitrović, Z., Paunović, N., Ilić, N., Tasić, N., Petronijević, I., Popović, D., & Stojanović, B. (2016). Comparative study of structural and electrical properties of Pr and Ce doped BiFeO₃ ceramics synthesized by auto-combustion method. *Journal of Alloys and Compounds*, 657: 866–872.
- Suharno, S., Hikam, M., Soegijono, B., & Toifur, M. (2014). Structural and dielectric properties of yttrium doped multiferroic bismuth ferrite (Bi_{1-x}Y_xFeO₃, x = 0, 0.18) synthesized by sol-gel method. ICOPIA 2014: 7th International Conference on Physics and Its Applications.
- Sun, Y., Wang, N., Yu, H., & Jiang, X. (2020). Metal-organic framework-based Fe/C@Co₃O₄ core-shell nanocomposites with outstanding microwave absorption properties in low frequencies. *Journal of Materials Science*, 55(17): 7304–7320.
- Sun, Y., Jia, H., Liu, J., Yu, H., & Jiang, X. (2020). Metal-organic framework-derived C/Co/Co₃O₄ nanocomposites with excellent microwave absorption properties in low frequencies. *Journal of Materials Science: Materials in Electronics*, 1–14. Doi: 10.1007/s10854-020-03721-z
- Suresh, S. (2015, April 7). *Thermogravimetric analysis*. [SlideShare]. Retrieved from: <https://www.slideshare.net/sureshselvaraj108/thermogravimetric-analysis>
- Suthar, L., Jha, V. K., Bhadala, F., Roy, M., Sahu, S., & Barbar, S. K. (2017). Studies on structural, electrical, thermal and magnetic properties of YFeO₃ ceramic. *Applied Physics A Materials Science & Processing*, 123(668): 1–9.
- Tripathy, S. N., Mishra, B. G., Shirolkar, M. M., Sen, S., Das, S. R., Janes, D. B., & Pradhan, D. K. (2013). Structural, microstructural and magneto-electric properties of single-phase BiFeO₃ nanoceramics prepared by auto-combustion method. *Materials Chemistry and Physics*, 141(1): 423–431.
- Uniyal, P., & Yadav, K. L. (2009). Pr doped bismuth ferrite ceramics with enhanced multiferroic properties. *Journal of Physics: Condensed Matter*, 21(405901): 1–7.
- Uniyal, P., & Yadav, K. L. (2008). Study of dielectric, magnetic and ferroelectric properties in Bi_{1-x}Gd_xFeO₃. *Materials Letters*, 62: 2858–2861.
- Valant, M., Axelsson, A.-K., & Alford, N. (2007). Peculiarities of a solid-state synthesis of multiferroic polycrystalline BiFeO₃. *Chemistry of Materials*, 19(22): 5431–5436.
- Van Aken, B. B., Palstra, T. T. M., Filipetti, A., & Spaldin, N. A. (2004). The origin of ferroelectricity in magnetoelectric YMnO₃. *Nature Materials*, 3: 164–170.

- Vanga, P. R., Mangalaraja, R. V., & Ashok, M. (2016). Sol-gel synthesis and characterisation of (Nd, Cr) co-doped BiFeO₃ nanoparticles. *Journal of Experimental Nanoscience*, 1–12. Doi: 10.1080/17458080.2016.1218556
- Vijayanand, S., Potdar, H. S., & Joy, P. A. (2009). Origin of high room temperature ferromagnetic moment of nanocrystalline multiferroic BiFeO₃. *Applied Physics Letters*, 94(182507): 1–3.
- Von Hippel, A. R. (1954a). *Dielectric Materials and Applications*. New York: John Wiley & Sons, Inc.
- Von Hippel, A. R. (1954b). *Dielectrics and waves*. New York: John Wiley & Sons, Inc.
- Wan Ab Rahman, W. N. (2012). *Physical interpretation of magnetic behavior in nickel zinc ferrite based on dielectric study*. Master Thesis, Universiti Putra Malaysia, Malaysia.
- Wang, D. H., Goh, W. C., Ning, M., & Ong, C. K. (2006). Effect of Ba doping on magnetic, ferroelectric, and magnetoelectric properties in multiferroic BiFeO₃ at room temperature. *Applied Physics Letters*, 88(21): 20–23.
- Wang, J., Neaton, J. B., Zheng, H., Nagarajan, V., Ogale, S. B., Liu, B., Viehland, D., Vaithyanathan, V., Schlom, D. G., Wahmare, U. V., Spaldin, N. A., Rabe, K. M., Wuttig, M., & Ramesh, R. (2003). Epitaxial BiFeO₃ multiferroic thin film heterostructures. *Science*, 299: 1719–1722.
- Wang, J., Scholl, A., Zheng, H., Ogale, S. B., Viehland, D., Schlom, D. G., Spaldin, N. A., Rabe, K. M., Wuttig, M., Mohaddes, L., Neaton, J., Waghmare, U., Zhao, T., & Ramesh, R. (2005). Response to comment on “epitaxial BiFeO₃ multiferroic thin film heterostructures.” *Science*, 307: 1203b.
- Wang, L. Y., Wang, D. H., Huang, H. B., Han, Z. D., Cao, Q.Q., Gu, B. X., & Du, Y. W. (2009). The magnetic properties of polycrystalline Bi_{1-x}Sr_xFeO₃ ceramics. *Journal of Alloys and Compounds*, 469: 1–3.
- Wang, N., Luo, X., Han, L., Zhang, Z., Zhang, R., Olin, H., & Yang, Y. (2020). Structure, performance, and application of BiFeO₃ nanomaterials. *Nano-Micro Letters*, 12(81): 1–23.
- Wang, Y. (2011). A giant polarization value in bismuth ferrite thin films. *Journal of Alloys and Compounds*, 509(41): L362–L364.
- Wang, Y. P., Zhou, L., Zhang, M. F., Chen, X. Y., Liu, J.-M., & Liu, Z. G. (2004). Room-temperature saturated ferroelectric polarization in BiFeO₃ ceramics synthesized by rapid liquid phase sintering. *Applied Physics Letters*, 84(10): 1731–1733.
- Wee, F. H., Soh, P. J., Abd Malek, M. F., & Hassan, N. (2012). Alternatives for PCB laminates: Dielectric properties' measurements at microwave frequencies. *Dielectric Material*, 91–112.

- Wei, J., Liu, Y., Bai, X., Li, C., Liu, Y., Xu, Z., Gemeiner, P., Haumont, R., Infante, I. C., & Dkhil, B. (2016). Crystal structure, leakage conduction mechanism evolution and enhanced multiferroic properties in Y-doped BiFeO₃ ceramics. *Ceramics International*, 42(12): 13395–13403.
- Weir, W. B. (1974). Automatic measurement of complex dielectric constant and permeability at microwave frequencies. *Proceedings of the IEEE*, 62(1): 33–36.
- Wen, F., Wang, N., & Zhang, F. (2010). Enhanced microwave absorption properties in BiFeO₃ ceramics prepared by high-pressure synthesis. *Solid State Communications*, 150(39–40): 1888–1891.
- Wenk, H.-R., & Bulakh, A. (2004). *Minerals: Their constitution and origin*. New York: Cambridge University Press.
- West, A. R. (2014). *Solid state chemistry and its applications*. Chichester: John Wiley & Sons, Ltd.
- William D. Callister, J., & Rethwisch, D. G. (2015). *Materials science and engineering*. Hoboken: John Wiley & Sons, Inc.
- Wongmaneerung, R., Padchasri, J., Tipakontitkul, R., Loan, T. H., Jantaratana, P., Yimnirun, R., & Ananta, S. (2014). Phase formation, dielectric and magnetic properties of bismuth ferrite-lead magnesium niobate multiferroic composites. *Journal of Alloys and Compounds*, 608: 1–7.
- Wu, J., Li, N., Xu, J., Zhou, S., Jiang, Y., & Xie, Z. (2015). Synthesis, phase diagram and magnetic properties of (1-x)BiFeO₃-xLaMnO₃ solid solution. *Journal of Alloys and Compounds*, 634: 142–147.
- Wu, J., & Wang, J. (2009). Effects of SrRuO₃ buffer layer thickness on multiferroic (Bi_{0.90}La_{0.10})X(Fe_{0.95}Mn_{0.05})O₃ thin films. *Journal of Applied Physics*, 106(054115): 1–5.
- Wu, Y.-J., Chen, X.-K., Zhang, J., & Chen, X.-J. (2012). Structural transition and enhanced magnetization in Bi_{1-x}Y_xFeO₃. *Journal of Magnetism and Magnetic Materials*, 324: 1348–1352.
- Xie, J., Feng, C., Pan, X., & Liu, Y. (2014). Structure analysis and multiferroic properties of Zr⁴⁺ doped BiFeO₃ ceramics. *Ceramics International*, 40(1): 703–706.
- Xu, J.-H., Ke, H., Jia, D.-C., Wang, W., & Zhou, Y. (2009). Low-temperature synthesis of BiFeO₃ nanopowders via a sol-gel method. *Journal of Alloys and Compounds*, 472: 473–477.
- Yan, F., Zhao, G., & Song, N. (2013). Sol-gel preparation of La-doped bismuth ferrite thin film and its low-temperature ferromagnetic and ferroelectric properties. *Journal of Rare Earths*, 31(1): 60–64.

- Yang, C.-H., Kan, D., Takeuchi, I., Nagarajan, V., & Seidel, J. (2012). Doping BiFeO₃: approaches and enhanced functionality. *Physical Chemistry Chemical Physics*, 14(46): 15953.
- Yang, C., Jiang, J.-S., Qian, F.-Z., Jiang, D.-M., Wang, C.-M., & Zhang, W.-G. (2010a). Effect of Ba doping on magnetic and dielectric properties of nanocrystalline BiFeO₃ at room temperature. *Journal of Alloys and Compounds*, 507: 29–32.
- Yang, K. G., Zhang, Y. L., Yang, S. H., & Wang, B. (2010b). Structural, electrical, and magnetic properties of multiferroic Bi_{1-x}La_xFe_{1-y}Co_yO₃ thin films. *Journal of Applied Physics*, 107(124109): 1–6.
- Yang, X., Zhang, Y., Xu, G., Wei, X., Ren, Z., Shen, G., & Han, G. (2013). Phase and morphology evolution of bismuth ferrites via hydrothermal reaction route. *Materials Research Bulletin*, 48: 1694–1699.
- Yao, Q. R., Shen, Y. H., Yang, P. C., Zhou, H. Y., Rao, G. H., Wang, Z. M., & Deng, J. Q. (2016). Structure, phase diagram and magnetic properties of Bi_{1-x}La_xFeO₃ solid solution. *Ceramics International*, 42(5): 6100–6106.
- Yasui, Y., Sato, K., Kobayashi, Y., & Sato, M. (2009). Studies of multiferroic system LiCu₂O₂:I. Sample characterization and relationship between magnetic properties and multiferroic nature. *Journal of the Physical Society of Japan*, 78(8): 1–5.
- Yin, T. T., & Mohamed Jelan, A. (2005). *Chemistry for matriculation semester 1*. Selangor: Penerbit Fajar Bakti.
- Yu, B., Li, M., Wang, J., Pei, L., Guo, D., & Zhao, X. (2008). Enhanced electrical properties in multiferroic BiFeO₃ ceramics co-doped by La³⁺ and V⁵⁺. *Journal of Physics D: Applied Physics*, 41(18): 1–6.
- Yu, J., Koshikawa, N., Arai, Y., Yoda, S., & Saitou, H. (2001). Containerless solidification of oxide material using an electrostatic levitation furnace in microgravity. *Journal of Crystal Growth*, 231: 568–576.
- Yuan, G. L., Or, S. W., & Helen Lai, W. C. (2007). Structural transformation and ferroelectric–paraelectric phase transition in Bi_{1-x}La_xFeO₃ (x = 0–0.25) multiferroic ceramics. *Journal of Physics D: Applied Physics*, 40: 1196–1200.
- Yuan, J., Hou, Z.-L., Yang, H.-J., Li, Y., Kang, Y.-Q., Song, W.-L., Jin, H.-B., Fang, X.-Y., Cao, M.-S. (2013). High dielectric loss and microwave absorption behavior of multiferroic BiFeO₃ ceramic. *Ceramics International*, 39: 7241–7246.
- Yuan, X.-P., Tang, Y.-K., Sun, Y., & Xu, M.-X. (2012). Structure and magnetic properties of Y_{1-x}Lu_xFeO₃ (0≤x≤1) ceramics. *Journal of Applied Physics*, 111(053911): 1–5.

- Zhang, H., Gao, B., Gui, Y. T., Wai, L. W., & Bai, L. (2013). Metal defects sizing and detection under thick coating using microwave NDT. *NDT&E International*, 60: 52–61.
- Zhang, S.-T., Zhang, Y., Lu, M.-H., Du, C.-L., Chen, Y.-F., Liu, Z.-G., Zhu, Y.-Y., Ming, N.-B. (2006). Substitution-induced phase transition and enhanced multiferroic properties of $\text{Bi}_{1-x}\text{La}_x\text{FeO}_3$ ceramics. *Applied Physics Letters*, 88(162901): 1–3.
- Zhang, S. T., Lu, M. H., Wu, D., Chen, Y. F., & Ming, N. B. (2005). Larger polarization and weak ferromagnetism in quenched BiFeO_3 ceramics with a distorted rhombohedral crystal structure. *Applied Physics Letters*, 87(262907): 1–3.
- Zhang, X., Sui, Y., Wang, X., Wang, Y., & Wang, Z. (2010). Effect of Eu substitution on the crystal structure and multiferroic properties of BiFeO_3 . *Journal of Alloys and Compounds*, 507(1): 157–161.
- Zhang, Y., Wang, Y., Qi, J., Tian, Y., Sun, M., Zhang, J., Hu, T., Wei, M., Liu, Y., & Yang, J. (2018). Enhanced magnetic properties of BiFeO_3 thin films by doping: Analysis of structure and morphology. *Nanomaterials*, 8(711): 1–13.
- Zheng, S., Wang, J., Zhang, J., Ge, H., Chen, Z., & Gao, Y. F. (2018). The structure and magnetic properties of pure single phase BiFeO_3 nanoparticles by microwave-assisted sol-gel method. *Journal of Alloys and Compounds*, 735: 945–949.
- Zhong, J., Heremans, J. J., Viehland, D., Yee, G. T., & Priya, S. (2010). Ferromagnetism and spin-glass-like behavior of BiFeO_3 nanoparticles. *Ferroelectrics*, 400(1): 3–7.
- Zhu, Y., Quan, C., Ma, Y., Wang, Q., Mao, W., Wang, X., Zhang, J., Min, Y., Yang, J., Li, X., Huang, W. (2017). Effect of Eu, Mn co-doping on structural, optical and magnetic properties of BiFeO_3 nanoparticles. *Materials Science in Semiconductor Processing*, 57: 178–184.